Recent Advances in Non-Enzymatic Electrochemical Detection of Hydrophobic Metabolites in Biofluids

Zahra Panahi , Luciana Custer , Jeffrey Mark Halpern

PII: S2666-0539(21)00027-8
DOI: https://doi.org/10.1016/j.snr.2021.100051
Reference: SNR 100051

To appear in: *Sensors and Actuators Reports*

Received date: 30 July 2021
Revised date: 24 September 2021
Accepted date: 27 September 2021

Please cite this article as: Zahra Panahi , Luciana Custer , Jeffrey Mark Halpern , Recent Advances in Non-Enzymatic Electrochemical Detection of Hydrophobic Metabolites in Biofluids, *Sensors and Actuators Reports* (2021), doi: https://doi.org/10.1016/j.snr.2021.100051

Recent Advances in Non-Enzymatic Electrochemical Detection of Hydrophobic Metabolites in Biofluids

Zahra Panahi, Luciana Custer, Jeffrey Mark Halpern[*]

Department of Chemical Engineering, University of New Hampshire,
Durham, New Hampshire 03824, United States

[*]Corresponding Author Email: Jeffrey.Halpern@unh.edu

Highlights:

- Representative surface modification technologies for the electrochemical detection of hydrophobic metabolites.
- Discussion of pH effect on sensing modality due to the complexation and free analyte detection
- Suggestion of rigorous testing in line with the concentrations found in practical biosamples

Graphical Abstract

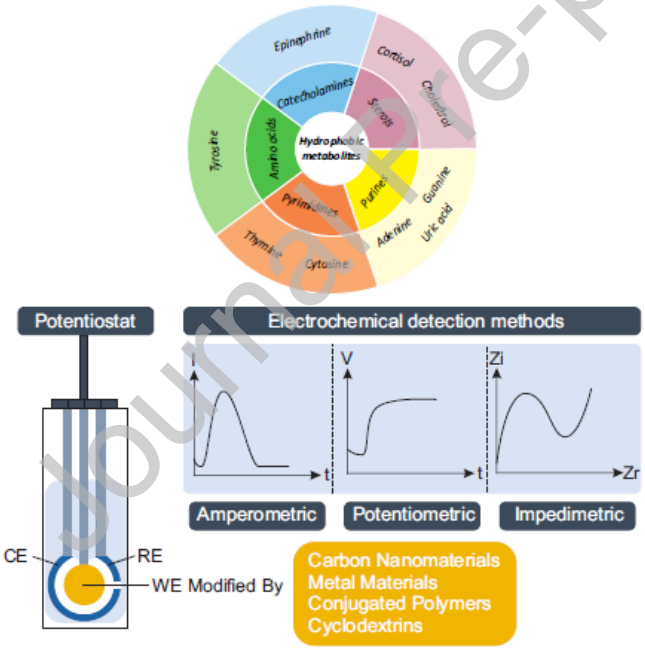

Abstract: This review focuses on recent advances in non-enzymatic electrochemical biosensors for detection of hydrophobic metabolites. Electrochemical approaches have been widely applied in many established and emerging technologies and a large range of electrochemical biosensors have been used for detection of various hydrophobic metabolites. Despite the progress made in this field, some problems still exist, specifically, electrochemical detection of hydrophobic biomarkers can be challenging in complex biological fluids. In this review, we have highlighted some of the most representative surface

modification technologies that have been employed in electrochemical biosensors to counter the problems of poor sensitivity and selectivity towards hydrophobic metabolites. The hydrophobic metabolites discussed in this review include uric acid, epinephrine, cortisol, cholesterol, tyrosine, adenine, guanine, cytosine, and thymine. This is followed by discussion on future research directions for electrochemical sensing of hydrophobic biomarkers.

Keywords:

electrochemical sensors; Hydrophobic analytes; Biofluids; Surface modifications; conjugated polymers; cyclodextrin; Metal Oxides

1. Introduction

Measurement of hydrophobic biomarkers (metabolites and proteins) has gained increasing attention in clinical research. Hydrophobic molecules are barely soluble in aqueous solutions which leads to very low concentrations in biological fluids. Therefore, sensitive and selective analysis of hydrophobic biomarkers is difficult in biological fluids.

Various methods including Raman spectroscopy, chromatography, and electrochemistry have been developed for detection of hydrophobic biomarkers in biological fluids. Surface enhanced Raman scattering (SERS) spectroscopy is an analytical platform that can be used for identification of hydrophobic biomarkers; however, the non-pretreated hydrophilic surface of metallic nanoparticle aggregates are typically not suitable for hydrophobic molecule detection [1]. High-performance liquid chromatography (HPLC) is among the most widely used methods for detection of hydrophobic biomarkers; however, sample preparation and extraction prior to the chromatographic analysis is essential. Solid phase extraction (SPE) and solid phase microextraction (SPME) are traditional solvent-free sample pretreatment techniques that can be coupled to HPLC. Despite being solvent-free, selection and preparation of proper SPE and SPME sorbent is crucial because the sorbent can significantly affect the selectivity and capacity of sample extraction [2]. Additionally, non-electrochemical techniques require expensive instrumentation, high maintenance costs, long sampling, and long analysis times. In contrast, electrochemical methods are more convenient for detecting biomarkers. In addition to fast response time and high sensitivity, electrochemical methods are cost effective and have more simple equipment.

Biosensors based on specific biorecognition elements such as antibodies or enzymes (immunoassays) exhibit high sensitivity and selectivity; however, they suffer from diverse restrictions: 1) Due to intrinsic instability of antibodies and enzymes, immunoassays are physically and chemically unstable, and they have low reproducibility. 2) Activity of immunoassays is greatly affected by experimental parameters such as temperature and pH. 3) Enzymes are expensive and complicated procedures are usually required for enzyme immobilization [3]. Over the last 5 years, there have been numerous artificial receptors and chemically modified surfaces developed to address the drawbacks of immune recognition or enzyme-based biosensors for detection of hydrophobic biomarkers.

Enzymes, antibodies, aptamers, and other naturally-based biorecognition elements are outside the scope of this review, and instead, we focus on surface modifications that promote non-enzymatic activity of hydrophobic analytes. Some of the most representative surface modification technologies for detection of five biological classes of hydrophobic metabolites (**Figure 1**) in the last 5 years are (i) carbon, (ii) metal, (iii) conjugated polymer, and (iv) cyclodextrin. The metabolites studied in this review

are biomarkers for a range of diseases. Understanding the chemical and biological behavior of these metabolites as well as their oxidation mechanism is essential to design appropriate biosensor technologies for point-of-need applications. This review attempts to provide an overview of hydrophobic metabolite biosensors, problems with existing biosensors, and future research opportunities in the area. Although this review focuses on non-enzymatic electrochemical detection of hydrophobic metabolites, a lot of progress has been made and been reviewed on improvements to non-enzymatic electrochemical sensing of hydrophilic metabolites [4,5] such as glucose [6,7] and dopamine [8].

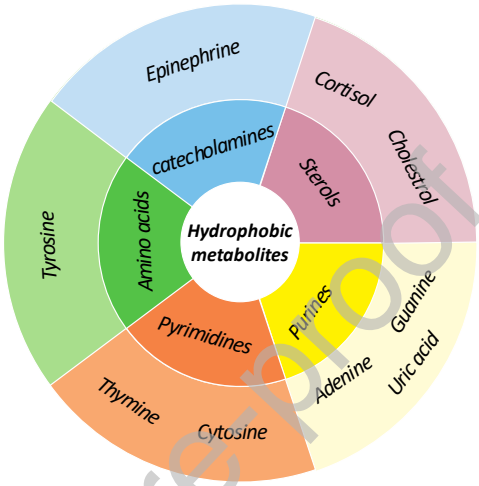

Figure 1. Different hydrophobic metabolites, defined as solubility less than 6 g/L, discussed in this review.

2. Importance and Difficulties in Detection of Hydrophobic Metabolites

For the purposes of this review, we have investigated electrochemical sensing platforms for several classes of hydrophobic small molecules with clinical relevance, *i.e.*, purine nucleobases (uric acid, adenine, and guanine), pyrimidine nucleobases (thymine and cytosine), an aromatic amino acid (tyrosine), a catecholamine synthesized from tyrosine (epinephrine), a sterol hormone (cortisol), and a hormone precursor (cholesterol). Understanding the biological and chemical behavior of these biomarkers is essential to design appropriate sensor technologies for point of care applications. Normal levels in biological fluids are summarized in **Table 1**.

Uric acid (UA) ($C_5H_4N_4O_3$) is the planar, heterocyclic end-product of purine metabolism in humans [9]. Although closely related to urea, which is very soluble, uric acid has very low water solubility and exists in concentrations close to the solubility limit in normal human blood [10]. Significant deviation from normal values is well correlated to disease, most notably gout [9,11] and Lesch-Nyhan disease [9]. UA mostly exists as a singly charged urate ion at physiological pH [12]. UA is deprotonated at a nitrogen atom and can use a tautomeric keto/hydroxyl group as an electron-withdrawing group, which allows for the formation of hydrogen bonds or electrostatic attractions between uric acid and sensor elements [12]. UA is electrochemically active and readily undergoes redox processes (**Figure 2A**) that can be quantitatively detected by electroanalytic techniques [13] but conventional electrodes struggle to differentiate UA from other species with similar oxidation potentials (e.g. dopamine, ascorbic acid, epinephrine) present in body fluids [14].

The cationic catecholamine epinephrine (EP) ($C_9H_{13}NO_3$), also known as adrenaline, is both a neurotransmitter and hormone [11]. EP plays a vital role in numerous processes, including glycogen metabolism [15], lipolysis in adipose tissue [15], and regulation of blood pressure and heart rate [16]. EP is also administered as a drug to treat bronchial asthma [17], cardiac arrest [18], anaphylaxis [17], and superficial bleeding [17], among other conditions. Catecholamines like EP have a short half-life in blood, resulting in very small detectable quantities [19]. Abnormal levels of EP may indicate the presence of cancer of the adrenal glands, with plasma levels as high as 5.5-54.6 nM noted in patients with pheochromocytoma [20]. The positive charge of EP at physiological pH permits electrostatic interactions between EP and sensor elements, while the benzene group may facilitate pi-stacking with aromatic sensor elements. Hydroxyl functional groups extending from EP may also be exploited for formation of hydrogen bonds. EP is easily oxidized and therefore highly electrochemically active (**Figure 2B**) but very low concentrations in body fluids and presence of interfering substances with similar oxidation potentials (e.g. ascorbic acid) makes EP determination challenging [18]. Additionally, the final product of epinephrine oxidation – epinephrinechrome – easily polymerizes to block electrode surfaces [18].

Cortisol ($C_{21}H_{30}O_5$) is a glucocorticoid (steroidal hormone) synthesized from cholesterol with significant long and short-term regulatory impact on immunologic, metabolic, cardiovascular, and homeostatic functions [19]. Even though roughly 90% of total cortisol is protein-bound, only free cortisol is considered biologically active and therefore of sensing interest [19]. Free cortisol levels peak before waking and fluctuate daily throughout bodily fluids, so timing of sample collection is important [19]. Saliva is particularly useful for cortisol assessment as it can be sampled repetitiously and non-invasively to monitor fluctuation. Low levels of cortisol may be caused by endocrine dysfunction (Addison's syndrome, hypopituitarism) but are also associated with stress-related disorders including chronic fatigue syndrome, fibromyalgia, and post-traumatic stress disorder [21]. Hypercortisolism may be caused by conditions like Cushing's syndrome or chronic stress and cause secondary/tertiary outcomes such as hypertension, insulin resistance, heart disease, and irreversible brain damage [19]. Cortisol is particularly challenging to electrochemically sense without antibodies or aptamers because it is uncharged at physiological pH and electrochemically inactive. An in-depth analysis of cortisol is not included in our review, which is focused on electrocatalytic activity involving modified surfaces, because cortisol has not had major advances in this area in recent years. However, various antibody-based sensors have been developed in recent years [22,23] and cortisol antibody functionalization strategies have recently been reviewed [24].

Cholesterol ($C_{27}H_3O_6$) is a major component of cell membranes and is the sterol precursor to steroidal hormones, vitamin D, and bile acids [25]. When packaged as a high-density lipoprotein (HDL), cholesterol can be excreted from the body through bile [25]. However, cholesterol is primarily transported in plasma as low-density lipoproteins (LDL) or very-low-density lipoproteins (VLDL) that tend to accumulate as fatty deposits in blood vessels, vastly increasing the risk for cardiovascular disease, stroke, and Type 2 diabetes [25]. Cholesterol also presents a challenge for electrochemical sensing without antibodies or enzymes due to its uncharged status at physiological pH and negligible electrochemical activity (**Figure 2C**).

Tyrosine (Tyr) ($C_9H_{11}NO_3$) is an aromatic, polar, non-essential amino acid that may be synthesized by hydroxylation of phenylalanine [26]. Elevated levels of tyrosine (>200 µM) may indicate disorders in the metabolic pathway such as phenylketonuria, tyrosinemia, and tyrosinosis [27]. Tyrosine, like most

amino acids, is weakly electrochemically active (**Figure 2D**) and generates poor responses at bare electrode surfaces. Tyrosine is also uncharged at physiological pH.

Table 1. Hydrophobic metabolite solubilities and normal concentrations

Analyte	Molecular Structure	Solubility in water (g/L)	Biological Fluid	Normal Ranges
Uric acid	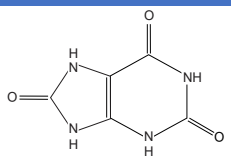	0.06	Serum	154.65 - 356.88 µM (premenopausal women)[28] 208.15 - 428.26 µM (men, menopausal women)[28]
			Urine	1.4-4.4 mM[29]
Epinephrine	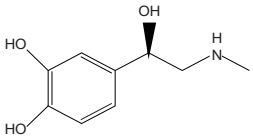	0.18	Serum	0 - 0.7643 nM[30]
			Urine	0.5 - 20 µg/24 hours[30] or 1.4-140 nM*
Cortisol	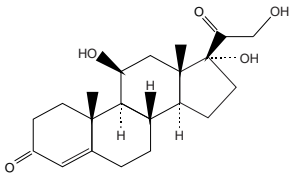	0.32	Blood	140 - 690 nM (sampled at 08:00)[30]
			Urine	8 - 51 µg/24 hours[31] or 11 – 281 nM*
			Saliva	Saliva: 3.5 - 27 nM (sampled at 08:00)[32]
Cholesterol	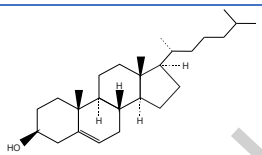	0.0018	Blood	<5.2 mM (Total cholesterol) [30] <2.6 mM (LDL) [30] >1 mM (HDL) [30] 0.1 – 1.7 mM (VLDL) [30]
Tyrosine	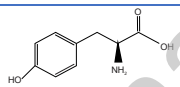	0.45	Blood	35 – 102 µM[26]
Adenine	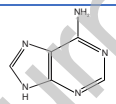	1.030	Plasma	Average concentration 2.7 ± 2.2 µM [33]
Guanine	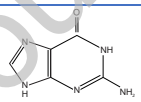	2.08	Plasma	Average concentration 0.4 µM [33]
Thymine	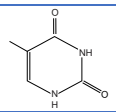	3.82	Plasma	Average concentration 2.4 µM [33]
Cytosine	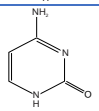	8	Plasma	Average concentration 6.4 ± 8.5 µM [33]

*assuming an average 24-hour urinary volume between 0.8-2.0 L

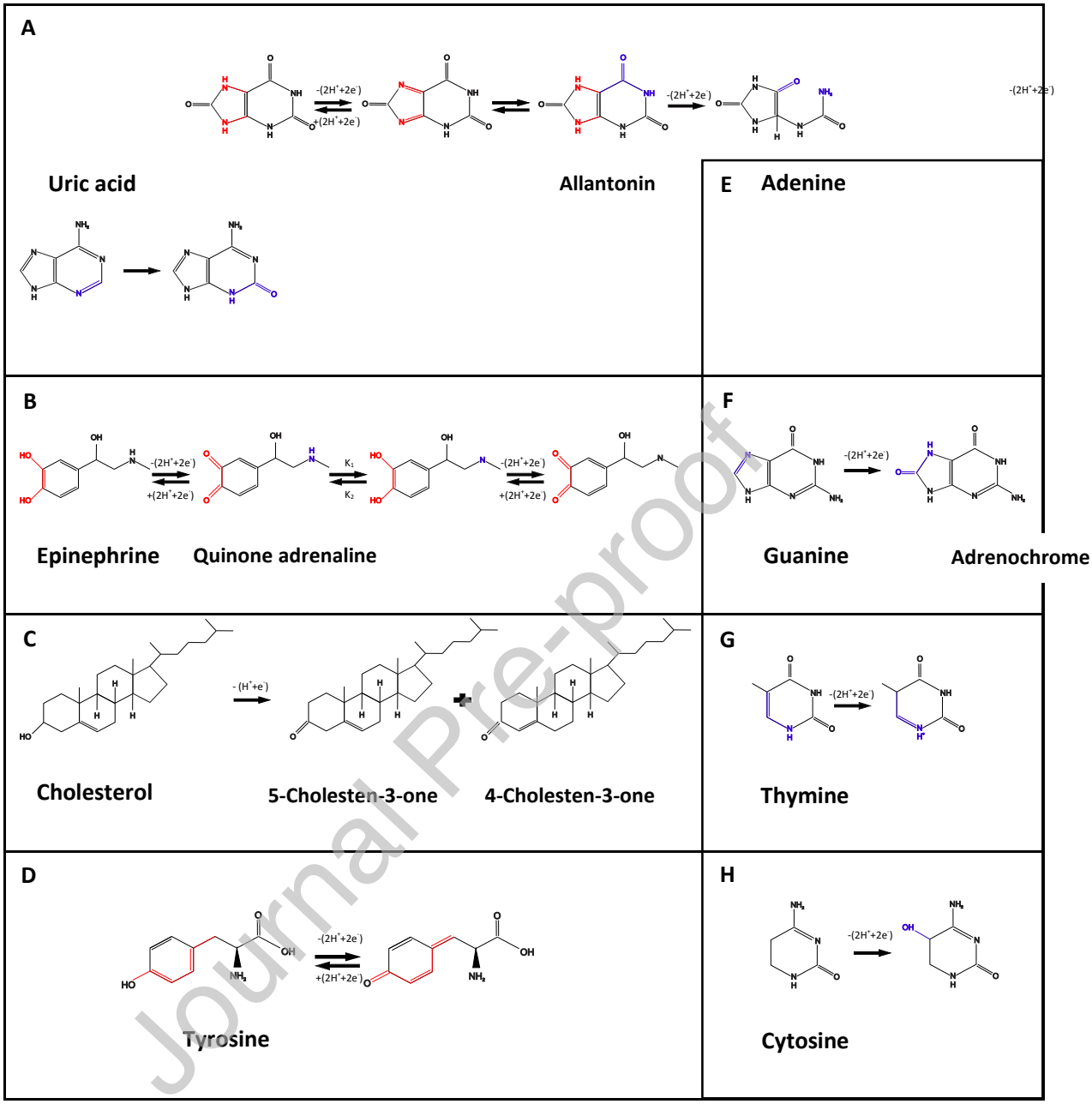

Figure 2. Proposed mechanisms for electrochemical oxidation of different hydrophobic metabolites: (A) Oxidation of uric acid on a polydopamine/polypyrrole (PDA/PPY) at 0.3 V vs. Ag/AgCl (in saturated KCl, 3M) [34]. (B) Oxidation of epinephrine on a zinc oxide/ferrocene functionalized graphene (ZnO/3D graphene@Fc) at 0.15 V vs. Ag/AgCl (contained 3 M KCl) [35]. The oxidation product of epinephrine (Quinone adrenaline) can be further oxidized to produce Adrenochrome at 1.15 V vs. Ag/AgCl (contained 3 M KCl) [35]**.** (C) Oxidation of Cholesterol on manganese oxide/graphene (MnO_2/GR) at -0.24 V vs. standard calomel [36] (D) Oxidation of tyrosine on cupric oxide oxide/ β cyclodextrin nanocomposite nafion (CuO/β-CD/Nf) at 0.69 V vs. Ag/AgCl [37]. (E) Oxidation of adenine on graphene oxide nanoribbons-chitosan (GONRs-CH) at 0.89 V vs. Ag/AgCl [38]. (F) Oxidation of guanine on GONRs-CH at 0.63 V vs. Ag/AgCl [38]. (G) Oxidation of thymine on GONRs-CH at 1.13 V vs. Ag/AgCl [38]. (H) Oxidation of cytosine on GONRs-CH at 1.27 V vs. Ag/AgCl [38].

Adenine and Guanine are purine nucleobases that form hydrogen bonds with pyrimidine nucleobases thymine and cytosine, respectively, to hold together two strands of DNA. Changes in concentration of these bases in fluids and tissues may reflect alterations in the activity of catabolic, anabolic, and other conversion enzymes and indicate disease states that disrupt normal purine and pyrimidine metabolism [39]. Furthermore, abnormal changes to thymine or a deficiency of thymine in DNA are linked to mutation or immune system irregularities that may contribute to symptoms of mental retardation, cancer, ageing, cardiovascular disease, renal failure and other diseases [40]. Nucleobases are considered electrochemically active (**Figure 2E-2H**) and all can be oxidized at solid electrodes [41].

While the focus of this review is on hydrophobic metabolites, there are many clinically relevant hydrophobic proteins. Proteins consist of long chains of amino acids and have the ability to fold to a specific functional three-dimensional shape. Because there are many types of amino acids, and their ordering determines how the protein chain will fold, protein molecules show characteristics of complex systems in terms of their structure, dynamics, and function [42]. Therefore, proteins are very different from small molecule metabolites and they have a different sensing paradigm. Due to the complex structure of proteins, sensing of hydrophobic proteins can be even more challenging than sensing of hydrophobic metabolites and will not be covered in the scope of this review.

3. Surface Modification Strategies

Various equilibrium and non-equilibrium transduction techniques have been used in electrochemical biosensors. Amperometric, voltametric, and impedimetric methods are mainly used in electrochemical biosensors to study the interfacial properties of electrode-electrolyte interface and the biorecognition events that happen in presence of analytes. In amperometric biosensors current resulting from the oxidation or reduction of an electroactive analyte is measured when a fixed potential is applied, whereas voltammetry measures the current response while varying potential. During impedimetric techniques such as electrochemical impedance spectroscopy (EIS), an AC potential is applied to the electrochemical cell and the current is measured. EIS biosensors are typically either based on the measurement of the change in charge transfer resistance (faradaic EIS) or capacitance (non-faradaic EIS).

Chronoamperometry (CA), differential pulse voltammetry (DPV), square wave voltammetry (SWV), linear sweep voltammetry (LSV), cyclic voltammetry (CV), and faradaic EIS have been among the most used electrochemical techniques for surface monitoring and hydrophobic biomarker detection over the past few years. Compared with CV and LSV, DPV results can provide improved selectivity for observing different redox processes [43]. SWV allows faster analysis times compared to other pulse techniques, such as differential pulse voltammetry or normal pulse voltammetry. Many of these methods such as DPV, SWV, and faradaic EIS are sensitive only to faradaic processes of interest and are used for direct measurement of peak potentials and peak currents of electrochemically active species. However, analysis of non-electroactive species can be achieved indirectly by measuring the signals of redox couples or other substances [44]. In this regard, cholesterol as a weak electrochemically active analyte, is a good test molecule for improving electrochemical sensor capabilities towards non-faradaic processes.

Electrocatalytic oxidation of cholesterol has been reported on biosensor surfaces such as MnO_2/GR/PGE [36] and GO-MIP [45] and the oxidation mechanisms of cholesterol in phosphate-buffered solution (PBS) are shown in **Figure 2C**. Despite the fact that the redox potential of cholesterol has been shown to be close to the redox potential of uric acid and acetic acid for the GO-MIP modified sensor, some researchers believe that cholesterol is not electrochemically active and redox couples like ferri/ferrocyanide[46] or electroactive probes like methylene blue [47] are needed as signal indicators.

In recent years, disposable carbon or metal screen-printed electrodes (SPEs) have been implemented for low-cost biosensors. SPEs are more suitable for point-of-care, electrochemical, on-site detection with low-cost. For example, a carbon SPE with a cortisol-alkaline phosphatase (AP) conjugate was developed to measure cortisol using SWV in PBS and saliva [48]. However, bare SPEs have a series of disadvantages, including poor sensitivity, instability, low reproducibility, large response times, high overpotential for electron transfer reactions, and small peak current [49,50]. Besides, the slow electron transfer kinetics of hydrophobic analytes, such as tyrosine, can limit the redox reaction rate and deteriorate biosensor performance [37].

Bare electrodes perform poorly because other interfering species present can be oxidized non-selectively. Surface modification can catalyze the oxidation of analytes to improve selectivity of biosensors in complex biological solutions. For example, the coexistence of interferents, such as dopamine, acetic acid, and epinephrine, can obscure the biosensor response to uric acid because they have very similar oxidation potentials. Additionally, oxidation products of the hydrophobic analytes can adsorb or electropolymerize on bare electrode surfaces, blocking further analyte oxidation and decreasing the reusability and reproducibility of these electrodes. Therefore, modifying different electrode surfaces is important to enhance sensitivity by increasing electron transfer rates, improve class-recognition selectivity in complex biological solutions, and prevent electrode fouling [51].

In this section, we will summarize some of the most effective surface modification technologies to address the problems of poor sensitivity and selectivity of biosensors. Various carbon materials (**Table 2**), metals (**Table 3**), conjugated polymers (**Table 4**), and cyclodextrins (**Table 5**) have an outstanding ability to combine with sensing elements and improve the electrochemical response in biosensors for detection of hydrophobic biomarkers.

3.1 Carbon Nanomaterials

Common carbonous materials, including graphene, graphene oxide, reduced graphene oxide, carbon nanotubes, carbon dots, carbon nanofibers, and carbon black, have drawn attention for electrochemical sensing of various metabolites. High electrical conductivity and high surface area of these materials mediate fast electron transfer between electroactive metabolites and electrode surface [52,53]. Besides this, carbonous materials can improve biosensor performance due to their wide potential window, high electrochemical stability, high mechanical resistance, and biocompatibility [52–54].

Incorporating carbonous materials into the surfaces can be challenging as simple drop-casting can result in unstable layers. Also, being too conductive and having high surface area poses problems in terms of controlling the electrical current and lack of selectivity. To address these problems, different polymers and sensing elements can be immobilized onto the carbonous materials through physical

adsorption and different covalent and non-covalent interactions. The choice of immobilization technology is significant. While physical adsorption is not a controllable process and non-covalent bindings may not be strong and stable enough, covalent modifications can cause changes in the properties of materials such as carbon nanotubes and graphene by disturbing their aromaticity [52,55]. Recent reviews have been written on different functionalization strategies and the design of various carbon materials [55–58].

Extensive applications of graphene in electrochemical detection of hydrophobic biomarkers such as uric acid [59], epinephrine [35] and tyrosine [60] have been reported. Graphene is a two-dimensional carbon material and a zero-bandgap semiconductor. Doping of graphene with nitrogen is mostly done to open up its band gap, enhance control of its electronic properties, and activate interaction between graphene surface and various biomarkers [59]. One of the most common ways to prepare N-dopped graphene sheets is the use of N-dominant substances such as urea. At high temperatures, urea decomposes into ammonia and forms N-dopped graphene via nitrogen containing functional groups of ammonia reacting with carbon atoms of graphene. **Figure 3A and 3B** show TEM images of graphene before and after nitrogen doping with urea [59]. This surface was used to develop a uric acid biosensor with sensitivity of 2.06 mA mM^{-1} cm^{-2}. However, in post-annealing the graphene with urea method surface area, the activity of graphene surface is likely to decrease due to uncontrolled C-N reactions and restacking of graphene films as it can be seen in **Figure 3B**. Other methods to synthesize N-dopped graphene such as decomposition of fumaric acid [61] or glycine [62] in the presence of sodium carbonate (Na_2CO_3) yielded thinner layers and higher surface area which may be helpful to increase sensitivity of N-dopped graphene biosensors.

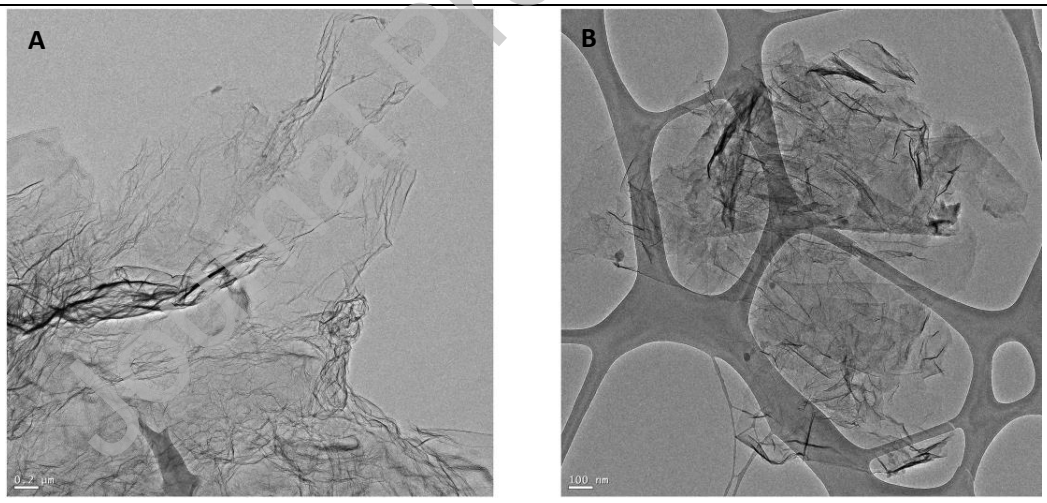

Figure 3. TEM images of A) graphene and B) N-doped graphene synthesized in the presence of uric acid [59]. Reprinted from A highly sensitive and selective biosensor based on nitrogen-doped graphene for non-enzymatic detection of uric acid and dopamine at biological pH value, 87, F. Foroughi, M. Rahsepar, and H. Kim, pp. 31-41, Copyright 2018, with permission from Elsevier.

Graphene oxide (GO) and reduced graphene oxide (RGO) which are among derivatives of graphene, find many applications for a wide variety of hydrophobic analytes such as uric acid [63,64], epinephrine[17], cortisol [23,65], cholesterol [45], adenine [38,63,66], guanine [38,63], cytosine [38], and thymine [38]. Oxygen containing groups on GO and RGO are useful for post-processing steps and enhance sensitivity of electrochemical biosensors by improving electron transfer rates and water

solubility [52,67]. Various electrochemical, thermal, and chemical methods are applied for conversion of GO into RGO. For example, RGO can be functionalized with metal nanoparticles such as ZnO that enhance electroactive surface area and electrochemical oxidation of different hydrophobic biomarkers (**Figure 4**) [64]. Another simple epinephrine biosensor was developed by combination of tetrahexahedral (THH) Au-Pd bimetallic nanocrystals with RGO nanosheets [17]. THH Au-Pd nanocrystals improved both electrocatalytic activity and conductivity of graphene. Further discussion of metallic elements is in section 3.2.

Carbon quantum dots (CQD) and graphene quantum dots (GQD) are electrochemically active species. Due to extremely small sizes and large surface area CQD and GQS have been recently used for detection of uric acid [68] and tyrosine [69], respectively. Besides, Quantum dots (QDs) can be synthesized with various functional groups and modification of surfaces with these materials allow electrochemical signal amplification and improvement of class-recognition selectivity [70,71].

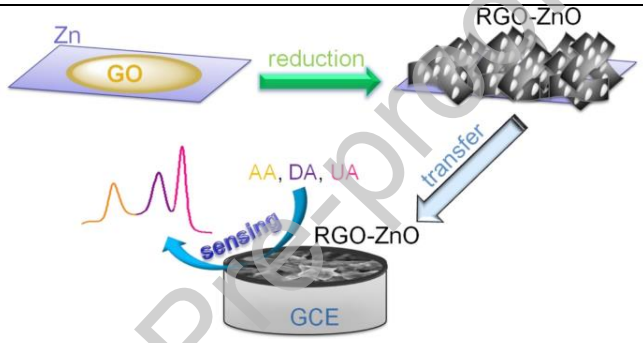

Figure 4. Schematic illustration of RGO–ZnO/GCE biosensor for detection of uric acid in the presence of ascorbic acid and dopamine [64]. Reprinted from One-pot facile fabrication of graphene-zinc oxide composite and its enhanced sensitivity for simultaneous electrochemical detection of ascorbic acid, dopamine and uric acid, 227, X. Zhang, Y.C. Zhang, and L.X. Ma, pp. 488-496, Copyright 2016, with permission from Elsevier.

Carbon nanotube (CNT) electrochemical biosensors are of great interest to researchers in recent years and can be classified into single-walled carbon nanotubes (SWCNT) and multi-walled Carbon nanotubes (MWCNT) sensors. CNTs consist of rolled graphene sheets and show different properties from graphene due to their unique structure. CNTs can enhance electrochemical activity of some biomarkers and have lower limit of detection (LOD), higher sensitivity, wider ranges of detection, and shorter detection times [58,72]. CNTs have been applied for recognition of many hydrophobic biomarkers, such as uric acid [73], tyrosine [27,74,75], and cholesterol [46]. Carbon nanotubes (CNTs) with small scale have been found to be able to increase the electrochemical sensitivity of numerous analytes [76]. A glycine polymer/multi-walled carbon nanotubes modified carbon paste electrode (Poly(Gly)/MWCNTs/CPE) was employed for detection of tyrosine [27]. Using this surface, a great sensitivity and accuracy was achieved in practical samples of human serum.

Carbon nanofibers (CNF) and CNTs have similar conductivity and stability; however, CNFs have larger surface area exposed to the solution and therefore have higher electron transfer rates. Transition metal dichalcogenides (TMDs) catalysts are also commonly supported on carbon nanofibers. As an example, a high-throughput three-dimensional WS_2 nanosheet/graphite microfiber hybrid electrode

biosensor was used for electrochemical detection of adenine and guanine in complex solutions and in vivo [77].

Other carbon materials such as carbon black, mesoporous carbon and fullerenes have been shown to be promising materials for biomedical analysis although their potential applications for detection of hydrophobic biomarkers are yet to be investigated.

There are some challenges with carbon based biosensors, especially with regard to insolubility of CNTs in aqueous solutions and reproducibility in producing identical batches of CNTs with high quality and minimal impurities [73,75]. However, combining the advantages of carbonous materials with different metals and polymers such as conjugated polymers and cyclodextrins gives a synergistic performance as electrode materials through which their advantages can outweigh their limitations.

Table 2. Carbon based biosensors

Analyte	Sensor	E-Chem method	Detection range* (µM)	LOD* (µM)	Medium	Ref.
Uric acid	RGO–ZnO/GCE	DPV	1-70	0.33	Plasma and urine	[64]
	N-doped graphene	CV	0-600	0.13	Serum	[59]
	P-GLY/GO	DPV	0.1-105	0.061	Urine	[63]
Epinephrine	Flower-like ZnO/3D graphene@Fc	DPV	0.02 - 216	0.0093	Serum	[35]
	Au-Pd/RGO	CV&DPV	0.001- 1000	0.0012	Serum	[17]
Cholesterol	GO-MIP	CV	$0.1\ 10^{-3}$ - 10,000	$0.1\ 10^{-3}$	Serum	[45]
Tyrosine	EFTA/ graphene /CPE	SWV	5 - 180	2	Serum and urine	[60]
	MCPE/COOH-MWCNT	CA	0.8-100	14 nM	Serum and cow's milk	[75]
	MW-FEs	DPV	25-750	8	Plasma and whole blood	[74]
Adenine	GONRs-CH	DPV	0.11-172	0.023	Buffer	[38]
	BODIPY functionalized SWCNT	DPV	4-20	2.91	Buffer	[76]
	WS_2/Graphite nanofiber	DPV	0.5-20	5×10^{-8}	Buffer	[77]
	TNFs/GONs/SPCE	CA	0.1-10	1.71 nM	Buffer	[66]
	P-GLY/GO	DPV	0.09-103	0.03	Urine	[63]
Thymine	GONRs-CH	DPV	6-855	1.330	Buffer	[38]
Guanine	GONRs-CH	DPV	0.013-256	0.002	Buffer	[38]
	BODIPY functionalized SWCNT	DPV	4-20	1.07	Buffer	[76]
	WS_2/Graphite nanofiber	DPV	0.5-20	9×10^{-8} M	Buffer	[77]
	P-GLY/GO	DPV	0.15-48	0.026	Urine	[63]
Cytosine	GONRs-CH	DPV	3.5-342	0.641	Buffer	[38]

*Detection range and LOD are typically determined in buffer and would likely be different in complex media.

3.2 Metal Materials

A wide variety of metals have been used to produce hydrophobic biosensors, including noble metals (e.g. Au [11,17,78], Pd [17]), transition metals (e.g. Co [78], Cu[79], W[80]), metal oxides/hydroxides (e.g. MnO_2[36], SnO_2 [81], $Zn(OH)_2$ [82], NiO [83]), metal chalcogenides (e.g. $FeTe_2$[9], CdSe[84]), metal organic frameworks (MOFs) [16], and polyoxometalates (POMs) [85,86]. Metallic materials have primarily been incorporated into these biosensors as a nonenzymatic electrocatalyst, providing crucial improvements in sensor sensitivity that in turn enable determination of biomarkers. The enhanced electrocatalysis of hydrophobic metabolites was achieved through several mechanisms: direct electron transfer mediation between metal and biomarker [87], coordination and activation of functional groups on the biomarker [87], improved electrostatic affinity between sensor and biomarker [11,18,85,88], enhanced mass transport due to expansion of the electrochemically active surface area [9,11,13,16,17,79–82,84–86,88] and/or intrinsic adsorptive properties of the metal [13,36,89]. Metals, especially transition metals with an abundance of unpaired d-orbital electrons, have multiple oxidation states and readily transition between oxidation states through electron transfer reactions with coordinating electrochemically active species [87]. This direct redox between metal and biomarker can facilitate faster electron transfer at lower oxidation potentials, as observed for the oxidation of epinephrine upon addition of copper nanoparticles to an Al_2O_3 nanofiber/graphene composite (**Figure 5a and 5b**) [79]. Since some hydrophobic metabolites like epinephrine and uric acid are electrochemically active and coexist with other electrochemically active species in complex media, metals present a useful option for enhancing sensitivity for these species creating some class-recognition type selectivity (**Figure 5C**).

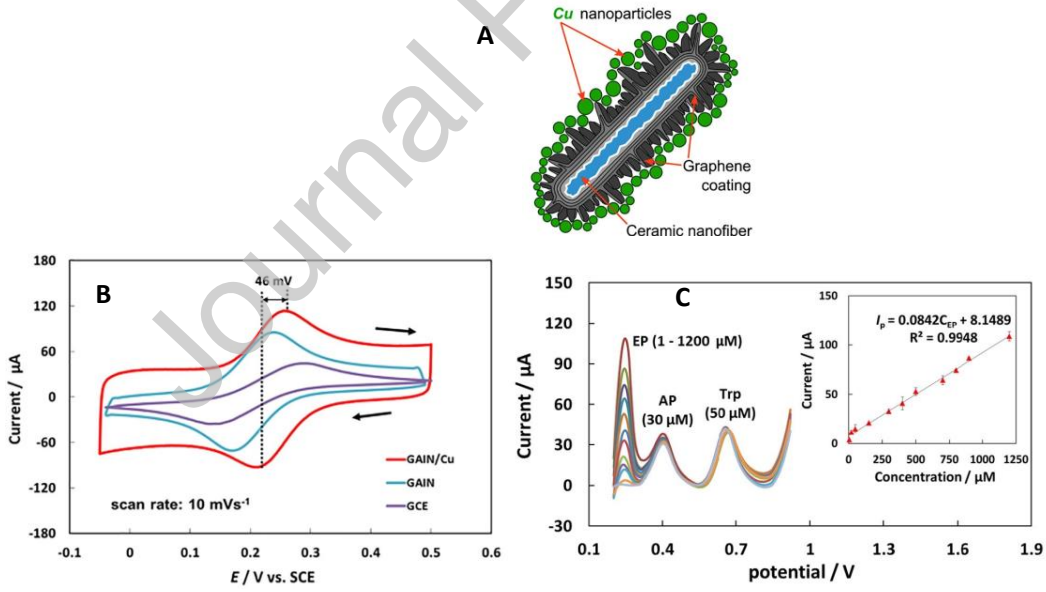

Figure 5. GCE modified with alumina/graphene/Cu composite for simultaneous detection of epinephrine, A) schematic illustration of alumina/graphene (GAIN) decorated by copper nanoparticles, B) CVs of GAIN, GAIN/Cu and GCE electrodes which shows GAIN/Cu modified surface mediates electron transfer at lower oxidation potentials, C) DPV measurement of epinephrine in presence of acetaminophen and tryptophan which shows high sensitivity and selectivity of biosensor [79]. Reprinted from Alumina/graphene/Cu hybrids as highly selective sensor for simultaneous determination of epinephrine, acetaminophen and tryptophan in human urine, 823, M. Taleb, R. Ivanov, S. Bereznev, S.H. Kazemi, I. Hussainova, pp. 184-192, Copyright 2018, with permission from Elsevier.

Interactions between two metals can also have an enhancing effect on biomarker redox processes, which could explain the enhanced oxidation of epinephrine upon addition of gold to a Schiff-base Iron (III) complex film [18]. However, Schiff-base complexes have been shown to degrade and corrode a metal oxide surface signifying limited long-term use of these in some applications [83]. Other examples of enhanced oxidation of uric acid with a second metal were gold added to a β-NiS/RGO composite [11] and a Co decorated hollow nanoporous carbon framework [78]. Enhanced oxidation of uric acid was also observed at α-$Ni_{0.75}Zn_{0.25}(OH)_2$ alloy nanoparticles compared to α-$Ni(OH)_2$ and $Zn(OH)_2$ alone [82]. Increased sensitivity to adenine and guanine was observed when ZnS was added to a CdS/GO modified electrode [88]. Some metals and metal composites have electrostatic affinity for the biomarkers of interest at tested pH that improve sensitivity for the target analytes. The negative charge of the Au/β-NiS/RGO [11], ZnS@CdS /GO [88], and Au/Schiff-base iron(III) [18] composites each attracted positively charged uric acid, adenine and guanine, and epinephrine, respectively. Conversely, the POM composite of $H_3PW_{12}O_{40}$/RGO contained positively charged surface groups that enhanced affinity for the negatively charged groups on tyrosine at tested pH [85].

If not directly participating in redox reactions with the biomarker, metal ions can bind functional groups on biomarkers with electron-donor properties [87] such as the amine groups on uric acid, adenine, guanine, cytosine, and thymine. Binding not only keeps the biomarker close to the electroactive surface but polarizes the functional group and activates adjacent sites on the molecule, thus promoting further interactions [87]. This effect may be responsible for the enhanced response of CdSe quantum dots in hollow extraction fibers towards uric acid versus just the hollow fibers, as each CdSe quantum dot binds at least one target analyte from solution and promotes oxidation [84]. While not necessarily specific to hydrophobic biomarkers, the binding to pull out of solution and activation of nearby sites is valuable when seeking higher sensitivities and wider peak separations for hydrophobic biomarkers containing Lewis base groups.

Metal nanostructures such as nanospheres, nanofibers, nanosheets, nanoclusters, and quantum dots may also improve sensitivity by increasing the electrochemically active surface area of the sensor, providing more accessible sites for redox. Morphology is key to this effect; although discal, cubic, and thorhombic Fe_2O_3 nanoparticles can all catalyze the oxidation of uric acid, the larger surface area/volume ratio and increased surface defects afforded by discal Fe_2O_3 nanoparticles yielded higher peak currents (**Figure 6**) [13]. Quantum dot core-shell nanostructures were of particular note, with ZnS@CdS producing even larger conductive surface areas than nanoparticles of the same metals [88]. Unfortunately, many metal nanoparticles are prone to agglomeration [13], and must be suitably dispersed (either by modifying synthesis technique or supporting on another structure) to reap the benefits of higher surface area.

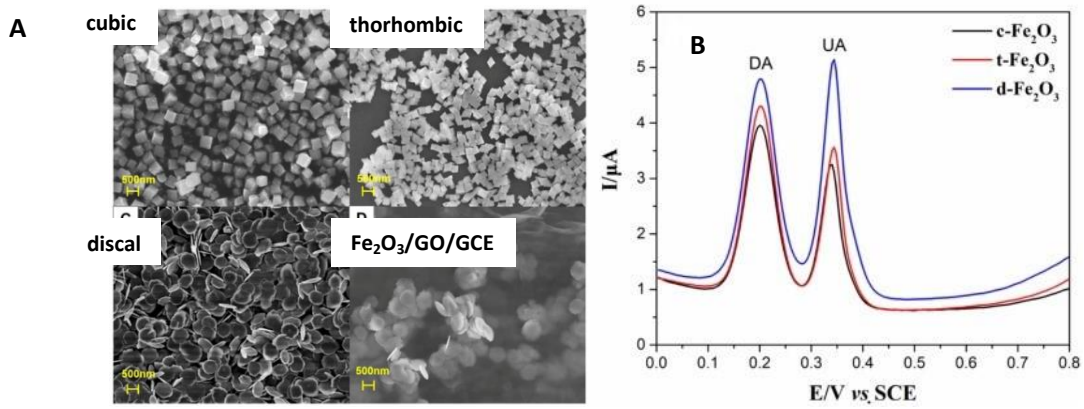

Figure 6. Effect of Fe_2O_3 nanoparticles' morphology on oxidation of uric acid A) SEM images of cubic, thorhombic, and discal Fe_2O_3 nanoparticles and a GO electrode modified with discal Fe_2O_3 nanoparticles, and B) DPV curves of GO electrode modified with cubic, thorhombic, and discal Fe_2O_3 nanoparticles which show higher electrocatalytic ability of discal Fe_2O_3 nanoparticles [90].

Table 3. Metal based biosensors

Analyte	Sensor	E-Chem method	Detection range (μM)*	LOD (μM)	Medium	Ref
Uric acid	Au/NiS/RGO/GCE	SWV	0.1-1000	0.006	Urine and serum	[11]
	Fe_2O_3/GO/GCE	DPV	10-100	0.0025	Urine and serum	[13]
	CdSe/ionic liquid/hollow polypropylene fibers/PGE	DPV	0.297-2970	0.083	Urine and serum	[84]
	$FeTe_2$/GPE	DPV	3-120	0.042	Urine and serum	[9]
	Au/Co/nanoporous hollow carbon framework/GCE	DPV	0.1-2500	0.023	Serum	[78]
Epinephrine	Au-Pd/RGO/GCE	DPV	0.001-1000	0.0012	Serum	[17]
	Al_2O_3/Cu/ graphene/GCE	DPV	1-1200	0.027	Urine	[79]
	CdO/PANI/ g-C_3N_4/GCE	DPV	0.05-1000	0.011	Serum	[16]
Tyrosine	$H_3PW_{12}O_{40}$/RGO /GCE	SWV	0.01-1.0 x 10^{-3}	2 x 10^{-6}	Serum	[85]
Cholesterol	PVIM-Co_5POM/MNC/ Filter paper electrode	DPV	1 x 10^{-8} -5000	1 x 10^{-9}	Serum	[86]
	MnO_2/PGE	DPV	1.2-24 x 10^{-3}	4.2 x 10^{-4}	Serum	[36]
Adenine	ZnS@CdS/GO/GCE	DPV	0.01-50	0.00181	Blood	[88]
	Fe_3O_4/GO/GCE	DPV	0.05-25	0.003	Urine	[89]
	$FeTe_2$/GPE	DPV	3-100	0.097	Urine and serum	[9]
Guanine	ZnS@CdS/GO/GCE	DPV	0.01-50	0.00145	Blood	[88]
	Fe_3O_4/GO/GCE	DPV	0.05-25	0.004	Urine	[89]
	$FeTe_2$/GPE	DPV	1-160	0.034	Urine and serum	[9]
	$Fe_2V_4O_{13}$/CPE	DPSV	0.5-60	0.032	Buffer	[91]
Cytosine	WO_2/W@C/GCE	DPV	1-3000	0.20	Urine and serum	[80]
Thymine	WO_2/W@C/GCE	DPV	1-4000	0.20	Urine and serum	[80]

*Detection range and LOD are typically determined in buffer and would likely be different in complex media.

Some metals (particularly iron oxides and metal chalcogenides) have notable impacts on mass transport due to their adsorptive abilities. Although pure unsupported iron oxide nanoparticles have poor electrical conductivity and are prone to agglomeration, the adsorptive ability of Fe_2O_3 and Fe_3O_4 were used to enhance the response of graphene oxide sheets towards uric acid [13] and

adenine/guanine [89] respectively. However, some metals have been shown to reduce mass transport rates, such as $Fe_2V_4O_{13}$ [91].

MOFs are highly tunable, porous, extended crystalline structures where metal cations or clusters called “nodes” are connected by organic “linker” ions or molecules [92]. MOFs can improve sensitivity with their electrocatalytically active metal nodes and selectivity by the modifiable pore sizes of the organic framework, often yielding wide detection ranges and very low limits of detection [92]. A CdO/carbon nitride/polyaniline MOF for epinephrine sensing demonstrates some of the advantages of MOFs with rapid diffusion, large surface area, improved peak separation between epinephrine and interferents, a higher oxidation current, and lower overpotential [16].

Although less explored in the literature, POMs are worth mentioning for their remarkably low limits of detection and wide range. POMs are molecular oxides containing oxygen and tens to hundreds of early transition metal atoms that can accept and release specific numbers of electrons without decomposing or changing structure [93]. POMs can vastly expand the electrochemically active surface area, enhancing electron transfer rate and sensitivity. A novel use of POMs was reported for nonenzymatic cholesterol sensing [86], yielding the lowest limit of detection with the widest range of the articles surveilled. The highly active sandwich POM, in combination with a PVIM+ ionic liquid support, showed cathodic peak shifts and an increase in reduction and oxidation currents of cholesterol, which is typically electrochemically inactive. Additionally, a POM/RGO/GCE sensor was reported for the determination of tyrosine [85], with electrostatic affinity for tyrosine as mentioned previously.

3.3 Conjugated Polymers

Conjugated polymers (CPs) are biocompatible polymeric materials with conjugated pi-orbital systems that may permit electron movement from end-to-end [94]. While in a pristine (neutral) state, CPs are poorly conductive [94,95]; conductivity of CPs is altered by several orders of magnitude via reversible oxidation (p-doping) or reduction (n-doping) of their pi-orbital system [94,95]. CPs can be polymerized in various conformations with unique behavior, including films [34,96–99], nanofibers/wires [34,100], nanospheres [14,101–104], and hydrogels [105]. CPs exhibit highly customizable structural, electronic, and optical properties that are sensitive to small perturbations, and therefore have been used for a variety of chemical sensing applications [94]. Common CPs for sensing include poly(thiophene)s like poly(3,4-ethylenedioxythiophene) (PEDOT), poly(aniline)s (PANIs), and poly(pyrrole)s (PPYs) [94]. PEDOT is among conducting polymers and can enhance sensitivity by mediating ion transport across the polymer-electrolyte interface. For example, **Figure 7** shows fabrication process of PEDOT/AuNP/MWCNT/GCE biosensor for uric acid detection which exhibited high sensitivity of 1.73 μA μM^{-1} cm^{-2}. Further, after three months, the response of PEDOT/AuNP/MWCNT/GCE biosensor only decays 8% of its initial response [106].

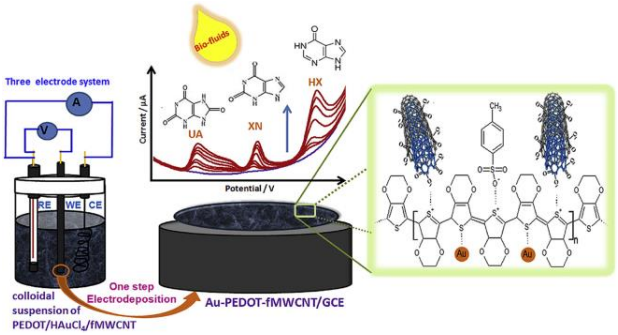

Figure 7. Schematic illustration of a PEDOT/AuNP/MWCNT/GCE biosensor for uric acid detection [106]. Reprinted from A simple electrochemical approach to fabricate functionalized MWCNT-nanogold decorated PEDOT nanohybrid for simultaneous quantification of uric acid, xanthine and hypoxanthine, 1114, S. Sen, P. Sarkar, pp. 15-28, Copyright 2020, with permission from Elsevier.

CPs can also improve the stability of sensors by providing functional groups for strong attachment to surfaces [14,96] and blocking surface fouling [97,107]. While some CPs like PPY or PANI are mechanically weak and degrade readily [96,102,107], others like PEDOT contribute decent mechanical strength as well as good thermal, environmental, and cycling stability [103]. CPs are also relatively cheap [94] and may be easily fabricated directly onto electrodes via electropolymerization [96,98]. However, CP only based sensors often have poor selectivity and are unsuited to discrimination of biomarkers in complex media outside of cross reactive sensor arrays [94]. Efforts to improve selectivity includes the integration of molecularly imprinted polymer concepts [108] or use of receptor monomers such as cyclodextrin [109].

As an element of biosensors, the large specific surface area [101], high conductivity [110], and fast redox activity [110] of CPs can improve sensitivity towards hydrophobic biomarkers (see **Table 4**). Many CPs like PANI have aromatic groups in their pi-orbital system that facilitate pi-pi stacking with aromatic hydrophobic molecules like uric acid [107], tyrosine [96], adenine [99], and guanine [99]. Charged groups on certain CPs at specific pH can change the overall charge of the composite to facilitate electrostatic interactions with hydrophobic biomarkers that are ionized at testing pH, such as uric acid [102], epinephrine [98], tyrosine [104], adenine [99], and guanine [99]; hydrogen bonding may also occur between proton donor regions of biomarkers and electronegatively rich groups of the CP that increase affinity for biomarkers [96,97,102] or weaken other bonds to enhance the likelihood of redox interactions [96]. Many CPs like PEDOT have more hydrophobic regions like repeated aromatic rings [100,102] or inclusion pockets [109] that can specifically interact with hydrophobic metabolites via hydrophobic interactions. Additionally, some CPs can catalyze the direct redox of a biomarker, such as poly(L-arginine) and epinephrine [98].

CPs are typically integrated into composites to great synergistic effect. For example, negatively charged carbon nanotubes form stable composites with positively charged PEDOT that have higher capacitance and enhanced mechanical properties as compared to electrodes modified with individual components [106]. Positively charged CPs have also been used to form p/n junctions with negatively charged materials like zinc oxide to substantially increase the magnitude of response towards epinephrine and uric acid [110]. CPs can enhance dispersal and prevent agglomeration of electrochemically active nanomaterials such as reduced graphene oxide [107], metal oxide nanoparticles [110], metal sulfide nanostructures [99,102], and noble metal nanoparticles [110,111], yielding more

homogeneous higher sensitivity constructs capable of selectivity. Carbon structures like reduced graphene oxide [110] or metal components [107] can compensate for the poor strength and stability of some CPs. However, compositing does not automatically yield better sensitivity; in particular, composites of CPs and 2-D carbon nanomaterials tend to have poorer (>0.5 µM) LOD [112,113].

While CPs are powerful due to their diversity of characteristics and synergy within composites, they require extensive optimization during polymerization/composite formation, doping, and sensing to maximize capabilities. Electro-polymerization conditions such as pH [14,111], solvent [100,111], supporting electrolyte [100], concentration of monomer [14,96,101], and choice of electrode substrate [14,100] influence the morphology and electrochemical properties of CPs and should be carefully selected for the biomarker of choice. Features such as thickness, permeation, and charge transport of CP films may be tuned by adjusting electrochemical parameters such as cycle number [96,97,111] and potential scan range [111].

Doping can be accomplished chemically or electrochemically, but electrochemical doping is preferable for reproducible fine tuning of oxidation state [94,95]. Different dopants produce CPs with varying characteristics [100]; sometimes other electrocatalytic hydrophobic materials like carbon nanotubes can be used as the dopant to enhance sensitivity [106]. Counterions are incorporated to compensate charges created by doping the polymer backbone. The type of counterion determines the character of local charge carriers along the polymer backbone [94], thereby determining ion exchange properties of the CP [95] and its interactions with ionized hydrophobic biomarkers. Further irreversible oxidation (over-oxidation) can turn some conductive CPs into insulating polymers [114], though recently over-oxidized PEDOT has been found to retain conductivity with the advantage of improved stability [100]. Over-oxidation may expose more hydrophobic regions of CPs such as PEDOT, facilitating hydrophobic interactions between the CP and un-ionized biomarkers for enhanced sensitivity and class-recognition selectivity [100]. CPs have also recently been electronically excited by electron beam irradiation, resulting in intermolecular cross linking or chain scission of the polymer [104] that manifests as altered electronic properties and mass transport behavior [101,104].

Table 4. Conjugated polymer based biosensors

Analyte	Sensor	detection method	Detection range (µM)*	LOD (nM)*	Medium	Ref.
Uric acid	Poly(DA)/AuNp/SPCE	DPV	10-350	0.1	Buffer	[14]
	Poly(DA)/PPY/GCE	DPV	0.5-40	110	Urine	[34]
	Poly(HQ)/crown ether/CNT/GCE	DPV	0.005-15	0.769	Serum	[97]
	PANI/ZnO/RGO/GCE	DPV	0.5-1000	122	Urine and serum	[107]
	PPY/β-NiS/SPE	SWV	0.02-1000	5	Urine and serum	[102]
	PEDOT/AuNp/ MWCNT/GCE	DPV	0.1-800	199.3	Urine and serum	[106]
	Ox-PEDOT/PGE	AdDPSV	0.01-20	1.3	Urine and serum	[100]
	PPY hydrogels/GCE	SWV	0.2-1000	46	Urine	[105]
	Poly(BCG)/AuNp/GCE	DPV	7.0-	4	Urine	[111]

			1500.0			
Epinephrine	Poly(L-aspartic acid)/RGO/GCE	SWV	0.1-110	25	Buffer	[98]
	Poly(BCG)/AuNp/GCE	DPV	4.0-903.0	10	Urine	[111]
	PPY/ZnO/AuNp/ RGO/GCE	DPV	0.6-500	60	Buffer	[110]
	EB-PPY/BSA/GCE	SWV	0.1-400	7.4	Buffer	[101]
Tyrosine	Poly(BCP)/ MWCNT/ CPE	CA	2-100	191	Buffer	[96]
	EB-PPY/BSA/GCE	SWV	0.1-400	5.9	Buffer	[101]
Cholesterol	PEDOT/taurine/SPE	CA	3-1000	950	Buffer	[103]
Adenine	PANI/MoS_2/CPE	DPV	0.05-1	6.3	Buffer	[99]
Guanine	PANI/MoS_2/CPE	DPV	1-100	4.5	Buffer	[99]

*Detection range and LOD are typically determined in buffer and would likely be different in complex media.

In addition to oxidation state, the electroactivity of CPs can be modified by protonation state. For certain CPs like PANI or PI, proton release and uptake are directly coupled to the oxidation or reduction of the polymer, such that changes in pH directly affect conductivity [95]. This feature of CPs, along with the ionization of several hydrophobic biomarkers at varying pH [96,100], necessitates experimentation with pH to determine optimal sensing conditions [14,96–104,106–111].

3.4 Cyclodextrins

Cyclodextrins (CD) consisting of six (α-CD), seven (β-CD), or eight (γ-CD) glucose units are oligosaccharides composed of a hydrophobic inner cavity and a hydrophilic outer surface. Because of their hydrophobic cavity they can make stable inclusion complexes with various hydrophobic guest molecules through Van der Waals forces, hydrogen bonding, and hydrophobic interactions. CDs have high molecular selectivity and have been used as molecular receptors in biosensors for detection of various hydrophobic biomarkers that match their cavity size [68]. In particular α-CD has a smaller cavity (inner radius 0.57 nm) and has been used for selective detection of adenine, guanine, and thymine [115]. β-CD (inner radius 0.78 nm) has been found to be the most efficient sterol-acceptor molecule, due to its inner cavity diameter which is consistent with the size of these molecules [46]. However, γ-CD (inner radius 0.95 nm) has a larger cavity which may not be suitable for selective detection of important biomarkers. For example it has been shown that sensitivity of β-CD/MWCNT sensor is higher than similar biosensors with α-CD and γ-CD for uric acid detection, thus demonstrating size of cyclodextrins is critical for small hydrophobic metabolite detection [116].

CD biosensors have good selectivity because different metabolites differ not only in terms of the nature and placement of a hydrogen-donor unit, but also in terms of the number of hydrogen donors. The host guest interaction energies between cyclodextrins and different guest molecules are always different, permitting the selective determination of the target molecules. In addition, steric hindrance controls the selectivity of cyclodextrin biosensors [109]. For example, tyrosine enantiomers (L-Tyr and D-Tyr) can both enter the β-CD cavity and make inclusion complexes with β-CD. However, due to different steric hindrance and hydrogen-bonding interaction between β-CDs and L-Tyr, β-CD:L-Tyr complex are shown to be more stable than β-CD:D-Tyr [69].

Carbon-based materials have been broadly used as supporting materials for electrochemical cyclodextrin biosensors to increase electron transfer rates and enhance electrochemical activity of these biosensors. Reduced graphene oxide has been used together with α-CD for detection of adenine, guanine, and thymine. α-CD ensures both more accessible active sites to capture analyte and RGO accelerates electron transfer leading RGO/α-CD to show high electrochemical activity [115]. Graphene quantum dots combined with ß-cyclodextrin for the fabrication of a tyrosine and uric acid biosensor and a β-CD/MWCNT surface has been incorporated for detection of uric acid [68,69].

One of the methods to improve sensitivity of layer-by-layer carbon/cyclodextrin biosensors is to optimize the interactions between carbon materials and cyclodextrins. **Figure 8A** shows different fabrication stages of a β-CD/Nafion-MWCNT biosensor for uric acid detection[116]. In this method, first, Nafion-ethanol solution was used to disperse pristine MWCNT and then β-CD was electropolymerized on Nafion-MWCNT film. However, the use of Nafion for MWCNT dispersion interferes with β-CD coupling to MWCNT. Alternatively, MWCNT–COOH (instead of unfunctionalized MWCNT) can be easily dispersed in aqueous solution and a layer of β-CD could be adsorbed directly on MWCNT layer [73]. By maximizing the interactions between MWCNT and β-CD sensitivity of biosensor increased from 2.11 to 4.28 μA mM^{-1} [73].

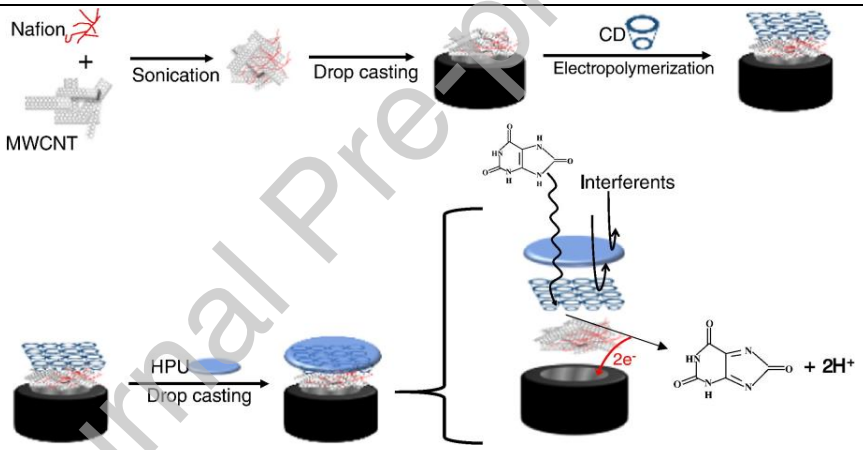

Figure 8. Schematic illustration of β-CD/Nafion-MWCNT for detection of uric acid [116].Reprinted from Electropolymerization of β-cyclodextrin onto multi-walled carbon nanotube composite films for enhanced selective detection of uric acid, 783, M.B. Wayu, L.T. DiPasquale, M.A. Schwarzmann, S.D. Gillespie, M.C. Leopold, pp. 192-200, Copyright 2016, with permission from Elsevier.

Table 5. Cyclodextrin based biosensors

Analyte	Sensor	Detection method	Detection range (µM)	LOD (µM)	Medium	Ref.
Uric acid	Poly (β-CD)/CQDs/GCE	DPV	0.3 - 200	0.01	Urine	[68]
	β-CD/ MWCNT–COOH	CA	100 - 700	100**	Buffer	[73]
	β-CD/RGO	DPV	0.08 - 150	0.026	Serum	[109]
Cholesterol	β-CD/MWCNTs/ SPCE	DPV	0.001 - 3	0.0005	Serum	[46]
Tyrosine	CuO/β-CD/ Nafion /GCE	CA	0.01 - 100	0.0082	Urine and serum	[37]
	β-CD/CQDs	CV-DPV	0.2 - 100	0.00607	Serum	[69]
	β-CD–GQD/GCE	DPV	0.1 - 1.5	0.1**	Buffer	[117]
Adenine	α-CD/RGO	DPV	10 - 50	0.1455	Serum	[115]
Thymine	α-CD/RGO	DPV	10 - 50	0.0529	Serum	[115]
Guanine	α-CD/RGO	DPV	10 - 50	0.0389	Serum	[115]

*Detection range and LOD are typically determined in buffer and would likely be different in complex media.
**Limit of quantification (LOQ)

However, one of the problems with cyclodextrin biosensors is associated with the immobilization of cyclodextrins on electrode surfaces due to their poor conductivity and high water solubility [109]. One solution is to introduce functional groups (such as –SH, $–NH_2$ and –COOH) on the CD, providing more effective binding sites. Covalent bindings between graphene and cyclodextrin can limit the amount of cyclodextrin immobilized on the surface and result in low sensitivity of biosensor. Furthermore, cyclodextrins are not conductive and cyclodextrin functionalized surfaces have lower conductivity. Therefore, introduction of cyclodextrins onto surface can decrease the sensitivity of sensors that are based on oxidation or reduction of electroactive analytes.

Dispersed cyclodextrin surfaces offer higher conductivity and perform better compared to cyclodextrin functionalized electrodes. Alternatively, competitive host-guest inclusion complexes between hydrophobic analytes and a redox indicator can be used to determine concentrations of analyte. For example, **Figure 9** shows that methylene blue can be replaced by cholesterol molecules because binding affinity of cyclodextrin and cholesterol is higher than cyclodextrin and methylene blue [118,119].

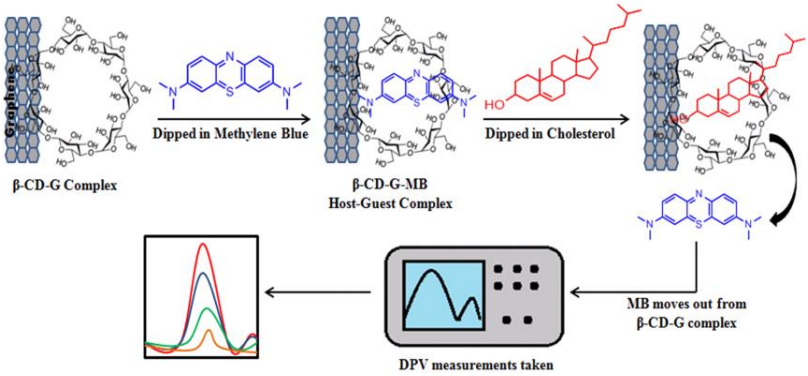

Figure 9. Schematic demonstration of β-CD/graphene platform for cholesterol detection [119]. Reprinted from Non-enzymatic electrochemical detection of cholesterol using β-cyclodextrin functionalized graphene, 63, N. Agnihotri, A.D. Chowdhury, A. De, pp. 212-217, Copyright 2015, with permission from Elsevier.

Therefore, using surfaces where cyclodextrin is complexed to a weekly hydrophobic self-assembled monolayer has the capability of creating a reusable and sensitive hydrophobic sensor [120]. A cyclodextrin mediated surface has the capability of overcoming the aforementioned challenges with surface functionalization with the added benefit of leveraging the competitive binding for a reusable surface.

4. Sensitivity, Selectivity, and Stability in Hydrophobic Metabolite Sensing

4.1. Sensitivity

Sensitivity is an important characteristic of the biosensor, and it is defined as the slope of the calibration curve [121]. Different surface modification methods are employed to enhance the sensitivity of biosensors; however, this parameter is often overlooked and receives less attention than LOD [122]. **Figure 10** demonstrates sensitivity of some of the reported amperometric biosensors, and the sensitivity of hydrophobic metabolite biosensors is usually between 1-10 μA $\mu M^{-1} cm^{-2}$ [9,34,80,106]. However, in case of an Au/Co/nanoporous hollow carbon framework/GCE surface for uric acid detection the sensitivity can be as high as 48.4 μA $\mu M^{-1} cm^{-2}$ [78] and MnO_2/PGE biosensor can detect cholesterol with sensitivity of 63869 μA $\mu M^{-1} cm^{-2}$ [123].

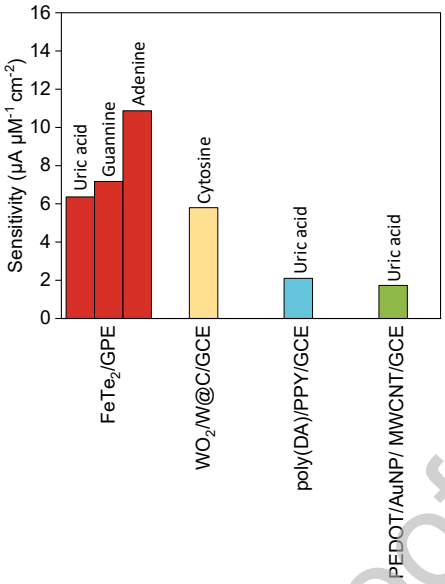

Figure 100. Sensitivity of some of the electrochemical biosensors for detection of hydrophobic metabolites [9,34,80,106]. Most of the reported amperometric biosensors detect hydrophobic metabolites with the sensitivity of 1-10 μA μM^{-1} cm^{-2}.

4.2 Selectivity

While biosensors with low sensitivity generate more false negatives, non-selective biosensors are likely to produce false positive results. Therefore, cross interference studies are performed to investigate the influence of potentially interfering compounds on biosensors response. These general points should be considered when selecting interfering compounds for selectivity experiments:

- Composition of biological solution: For example, uric acid as an important organic constituent of urine can interfere with various hydrophobic metabolites detection. Therefore, uric acid should always be tested when the biosensors are developed to detect analytes in urine.
- Electrochemical detection technique: For example, in amperometric biosensors various electroactive molecules can be oxidized or reduced at the surface. Therefore, all electroactive species that coexist with target analyte can be potential interferents.
- Nature of modified surface: For example, cyclodextrins can make inclusion complexes with various hydrophobic guest molecules. Therefore, it is important to note the presence of coexisting hydrophobic molecules in the solution.
- Glucose, cysteine, acetaminophen, ascorbic acid, and citric acid are among the most possible interfering analytes during uric acid selectivity studies [9,11,13,14,34,63,64,68,73,78,97,100,102,105–107,109]. The presence of acetaminophen can be problematic for uric acid detection and response of β-CD/ MWCNT–COOH was shown to this analyte [73]. Besides, uric acid has similar oxidation potential with some other hydrophilic or hydrophobic metabolites such as dopamine and epinephrine.

These general points can be expanded to specifics as detailed in **Table 6** and below:

Table 6. Common interfering components that are tested to evaluate selectivity of biosensors

Analyte		Sensor	Interferents Tested	Ref.
Uric acid	Carbon	RGO–ZnO/GCE	glucose, cysteine, NaCl, KCl, $CaCl_2$, $MgSO_4$, Fe $(NO_3)_3$	[64]
		N-doped graphene	glucose, acetaminophen, urea	[59]
		P-GLY/GO	glucose, sucrose, L-glutamic, ascorbic acid, epinephrine	[63]
	Metal	Au/NiS/RGO/GCE	glucose, citric acid, cysteine, KCl, Na_2SO_4, $NaNO_3$	[11]
		Fe_2O_3/GO/GCE	ascorbic acid, citric acid, alanine, glutamic acid, lysine	[13]
		$FeTe_2$/GPE	ascorbic acid, glucose, citric acid, cysteine, Na^+, K^+, Cl^-	[9]
	CP	Poly(DA)/PPY/GCE	glucose, bilirubin, ascorbic acid, creatine, xanthine, hydrogen peroxide, nitrite	[34]
		Ox-PEDOT/PGE	ascorbic acid, serotonin, dopamine	[100]
	CD	β-CD/ MWCNT–COOH	sodium nitrite, oxalic acid, and glucose, acetaminophen	[73]
		β-CD/RGO	ascorbic acid, dopamine, citric acid, cysteine, glucose KCl, NaCl, $MgCl_2$, $CaCl_2$	[109]
Epinephrine	Carbon	Flower-like ZnO/3D graphene@Fc	uric acid, ascorbic acid, folic acid, glucose, tyrosine, tryptophan, NADH, xanthine, adenosine, guanosine	[35]
		Au-Pd/RGO	ascorbic acid, dopamine, urea, glucose, KCl	[17]
	Metal	Al_2O_3/Cu/graphene/GCE	urea, glucose, dopamine, uric acid, $FeCl_3$, $MgCl_2$, KCl, Na_2SO_4, NH_4Cl, NaCl, H_2O_2,	[79]
		CdO/PANI/g-C_3N_4/GCE	ascorbic acid, dopamine, uric acid, glucose, tryptophan, tyrosine	[16]
		EB-PPY/BSA/GCE	ascorbic acid, folic acid, dopamine, uric acid, KCl	[101]
Cholesterol	Carbon	GO-MIP	ascorbic acid, uric acid, glucose	[45]
	Metal	PVIM-Co_5POM/MNC/ Filter paper electrode	glucose and uric acid	[86]
		MnO_2/PGE	glucose, glycine, uric acid, cholecalciferol, ascorbic acid, estradiol, NaCl, KCl, $MgCl_2$	[36]
	CP	PEDOT/taurine/SPE	glucose, lactic acid, uric acid, glycerol, ascorbic acid, dopamine	[103]
	CD	β-CD/MWCNTs/ SPCE	glucose, ascorbic acid, uric acid	[46]
Tyrosine	CP	Poly(BCP)/MWCNT/ CPE	ascorbic acid, uric acid, dopamine	[96]
	CD	β-CD/CQDs	tryptophan, glutamine, threonine, alanine, arginine, valine, serine, methionine, lysine	[69]
Adenine, Guanine, Thymine, and Cytosine	Carbon	BODIPY functionalized SWCNT	ascorbic acid, caffeine, Cr^{3+}, Ni^{2+}, Zn^{2+}, Cu^{2+}, Fe^{3+}, Ca^{2+}, Mg^{2+}, SO_4^{2-}, NO_3^-, Cl^-	[76]
		WS_2/Graphite nanofiber	Mg^{2+}, Ca^{2+}, Zn^{2+}, Cl^-, NO_3^-, SO_4^{2-}	[77]
	Metal	ZnS@CdS/GO/GCE	glucose, thymine, alanine, uric acid, ascorbic acid glycine, methionine, leucine, arginine, folic acid, tryptophan, and inorganic ions such as Cl^-, K^+, Na^+, Mg^{2+}, NO_3^-, Ca^{2+}, Zn^{2+}, SO_4^{2-}	[88]
		Fe_3O_4/GO/GCE	glucose, glycine, K^+, Ca^{2+}, Zn^{2+}, Na^+	[89]
		WO_2/W@C/GCE	glucose, sucrose, glutamic acid, adenine, guanine, uric acid, dopamine, ascorbic acid, Zn^{2+}, $Cu^{2+}$and Ca^{2+}, Na^+, Mg^{2+}, K^+	[80]
	CD	α-CD/RGO	ascorbic acid, uric acid, glucose	[115]

- In the case of epinephrine, biosensors response to ascorbic acid, glucose, dopamine, and tyrosine should be investigated [16,17,35,79,98,101,110]. Besides, tryptophan and guanosine have shown weak oxidation peaks in response to ZnO/3D graphene@Fc biosensor which was developed for epinephrine detection [35].
- In order to investigate the selectivity of biosensors toward cholesterol, the biosensors response to glucose, ascorbic acid, estradiol, and glycerol should be tested [36,45,46,86,103].
- To assess the performance of tyrosine biosensors in biological fluids such as plasma and urine, in addition to common interferents such as uric acid and ascorbic acid, the influence of amino acid enantiomers such as tryptophane, threonine, glutamine, and methionine should be studied. It has been shown that tryptophan and methionine enantiomers can be oxidized by β-CD/CQDs surface [69].
- Purine nucleobases (adenine and guanine) and pyrimidine nucleobases (thymine and cytosine) are usually determined simultaneously. Therefore, it is important for biosensors to show distinct oxidation peaks for each of these analytes. Additionally, the interference effect of uric acid, ascorbic acid, glucose, sucrose, and inorganic ions such as Zn^{2+}, Cu^{2+}, Ca^{2+}, Mg^{2+}, SO_4^{2-}, NO_3^-, and Cl^- should be investigated [66,76,77,80,88,89,115].

4.3 Stability

Short-term (or sensing) stability as well as long-term (or storage) stability are widely used to describe biosensor performance. Sensing stability evaluates the effect of surface fouling on biosensors response. For example, constant amperometric response of MCPE/COOH-MWCNT for 20 min suggested the biosensor was stable in solution during sensing of tyrosine [75]. Additionally, after 80 continuous DPV sweeps using ZnS@CdS/GO/GCE surface, adenine and guanine oxidation peak currents only dropped to 90.7 and 91.2 % of their original values, respectively [88]. Similarly, 25 CV cycles were repeated to show antifouling property of poly(HQ)/crown ether/CNT/GCE surface for uric acid detection [97].

Moreover, long storage stability of biosensors is required for clinical applications. **Figure 11** represents storage stability of various biosensors in dry room temperature (**Figure 11A**), dry low temperatures (**Figure 11B**), and buffer solutions (**Figure 11C**) where the biosensor retains at least 90% of their original response after storage period.

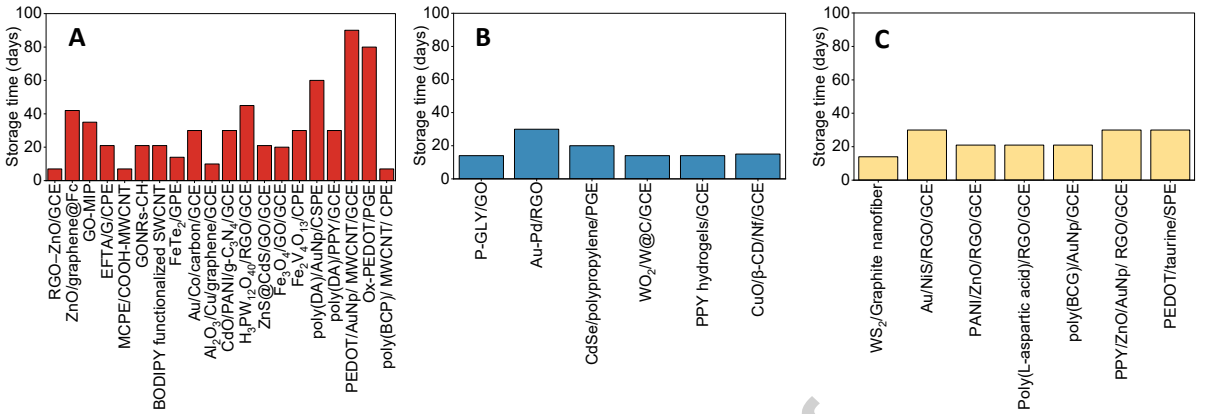

Figure 111. Storage stability of various biosensors in A) dry room temperature [9,14,16,34,35,38,45,60,75,76,78,79,85,88,89,91,96,100,106], B) dry low temperatures [17,37,63,80,84,105], and C) buffer solutions [11,77,98,103,107,110,111]. PEDOT/AuNp/ MWCNT/GCE was stable at room temperature for 3 months and had the longest storage stability. Also, the average storage time values of reviewed biosensors, [9,11,14,16,17,34,35,37,38,45,60,63,75–80,84,85,88,89,91,96,98,100,103,105–107,110,111], kept at room temperatures, low temperatures, and in buffer solutions were reported to be 31, 18, and 20 days, respectively.

5. Existing Problems and Future Directions

As summarized in **Tables 2-5**, many biosensors have been developed for sensitive detection of hydrophobic biomarkers with significant LOD. For example, for uric acid, the LOD can be as low as 0.1 nM. Considering the normal range of uric acid in serum (154.65-428.26 µM) and urine (1.4-4.4 mM), the biosensor might seem to be suitable for assessment of the concentrations of analyte in serum and urine [121]. However, in many cases the reported limit of detections in buffer solutions cannot be equivalently compared and especially cannot be expected in real samples for various reasons:

- There is currently no well-defined and validated procedure for calculation of the LOD of electrochemical biosensors. The International Union of Pure and Applied Chemistry (IUPAC) and The International Council for Harmonization of Technical Requirements for Pharmaceuticals for Human Use (ICH) have provided guidelines for LOD determination [124,125]. Depending on whether the procedure is instrumental or non-instrumental, LOD of electrochemical biosensors can be calculated based on visual examination, signal to noise ratio, the standard deviation of the blank, or the calibration curve, which provide different results.
- While standard protocols usually require at least 20 replicates for determination of LOD, LODs are usually reported based on only 3 or even less measurements. Thus, it is questionable to what extent these low LODs can be reproduced.
- The discrepancy between LOD of biosensors in buffer and complex biological solutions is often attributed to interfering competing analytes that are only present in complex media. However, the different states of analytes in buffer and complex solutions may also cause the discrepancies.

It is crucial to make a distinction between free and complexed (bound) biomarkers. While in buffer solutions the hydrophobic biomarkers exist in their free state, in complex biological solutions hydrophobic biomarkers, like cholesterol, are often stored or held together with hydrophilic molecules by noncovalent forces. In other words, complexed biomarkers must overcome the interactions of their surrounding hydrophilic molecules and flow into the solution prior to interacting with the sensors surface. As such, it will be beneficial to first employ the developed biosensors to measure complexed biomarkers in buffer solutions and then evaluate the biosensors in complex solutions and investigate the effect of the analyte state and interfering molecules in the complex solution independent from each other.

In our literature assessment, we have found pH effects on hydrophobic analyte detection extremely important to the sensitivity and selectivity of measurement because of the pH effect on sensing modality, differences in charge state of the analyte, and pH effects on the complexation of hydrophobic analytes. Testing the biosensors response to complexed analytes in buffer solutions can provide researchers more accurate data regarding the effects of various experimental parameters such as pH on sensors function. Adjusting the pH of the complex solution through sample preparation typically has great impacts on electrochemical biosensors performance for detection of hydrophobic biomarkers. First, functional groups of many hydrophobic biomarkers can potentially undergo acid-base reactions and the hydrophobicity and solubility of many hydrophobic biomarkers varies significantly in different pH solutions. For example, while guanine is negligibly soluble in neutral solutions, its solubility varies with pH due to its dissociation or protonation [126]. Uric acid [127], epinephrine [128], and tyrosine [129] can also be present in different forms and charged states and their solubility in aqueous solutions depend on the pH of the solution. Second, different pH results in different interfacial behaviors of biosensors. Also, many biomarkers have different peak oxidation potential in different pH solutions. Finally, pH of the solution affects the dominance of side reactions such as hydrogen and oxygen evolution in electrochemical measurements.

Based on literature assessment, there appears to be no universal way of reporting pH effects on complexed-analyte versus free-analyte in solution, and therefore, we encourage researchers to consider reporting both cases separately. Currently, the researchers gather their pH data based on free analytes in buffer solutions, most often phosphate buffer, however; testing the complexed analytes in buffer yields more valid data because it avoids free-analytes bias. We created the following decision and reporting map (**Figure 12**) to aid researchers on the different types of solutions and complexation that could occur within a sample. Worth noting is within selectivity experiments, competing analytes should also be tested and ideally show no response to the testing pH effect with free analyte.

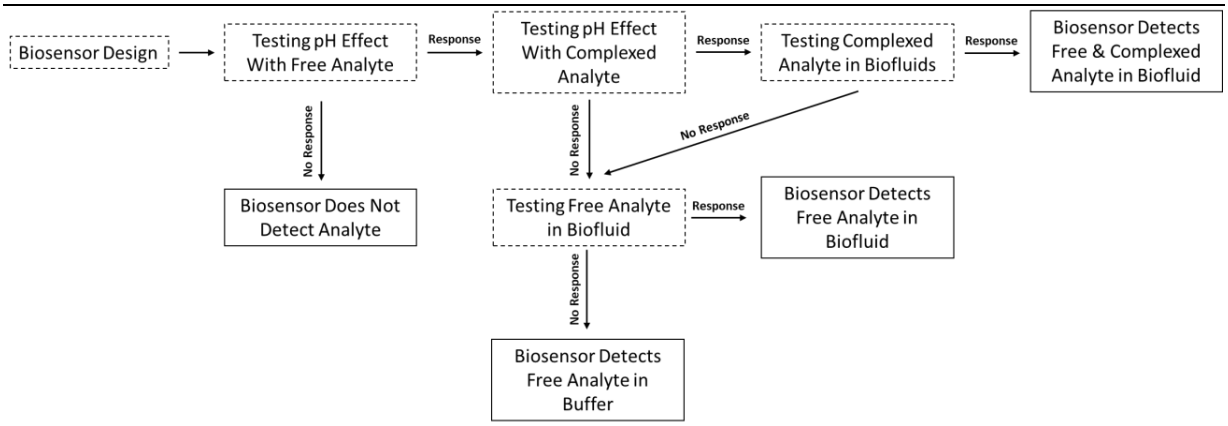

Figure 12. Decision map that can be used to design hydrophobic metabolites sensing experiments.

6. Conclusion

In conclusion, hydrophobic metabolites are extremely important in assessing biofluids. Progress is clearly observed in the increased sensitivity of electrocatalytic surfaces towards hydrophobic analytes. However, challenges remain in selectivity of specific analytes and the ability to assess the true concentration of free versus complexed analytes. To improve accuracy, reliability, and commercialization of biosensors we propose the decision map shown in **Figure 12** for testing of hydrophobic metabolites. This procedure includes testing the biosensor response to free and complexed analytes in buffer and investigation of pH effect on the biosensor response, which may improve systematic discovery of ideal sensing conditions and ameliorate the difficulties associated with measuring such low concentrations in aqueous fluids. Additionally, we suggest rigorous testing and reporting of complex media sensing capabilities that are in line with the concentrations found in practical samples such as undiluted or diluted biofluids.

7. Abbreviations

SERS: Surface enhanced Raman spectroscopy
HPLC: High performance liquid chromatography
SPE: Solid phase extraction
SPME: Solid phase microextraction
UA: Uric acid
EP: Epinephrine
Tyr: Tyrosine
CA: Chronoamperometry
EIS: Electrochemical impedance spectroscopy
DPV: Differential pulse voltammetry
AdDPSV: Adsorptive differential pulse stripping voltammetry
SWV: Square wave voltammetry
LSV: Linear sweep voltammetry
CV: Cyclic voltammetry
GO: Graphene oxide
GON: graphene oxide nanosheet
RGO: Reduced graphene oxide
CQD: Carbon quantum dot
GQD: Graphene quantum dot
CNT: Carbon nanotube
SWCNT: Single-walled carbon nanotube
MWCNT: Multi-walled carbon nanotube
LOD: Limit of detection
TMD: Transition metal dichalcogenides
MOFs: Metal organic frameworks
CP: Conjugated polymer
POMs: Polyoxometalates
PEDOT: Poly(3,4-ethylenedioxythiophene)
PANI: Poly(aniline)
PPY: Poly(pyrrole)
CD: Cyclodextrin
IUPAC: International Union of Pure and Applied Chemistry
ICH: International Council for Harmonization of Technical Requirements for Pharmaceuticals for Human Use
GCE: Glassy carbon electrode
P-GLY: Poly(glycine)
MIP: Molecular imprinted polymer
EFTA: Ethyl 2-(4-ferrocenyl-[1,2,3]triazol-1-yl) acetate
CPE: Carbon paste electrode
MCPE: Modified carbon paste electrode
MW-Fes: Filtered multi-walled carbon nanotubes
GONRs-CH: Graphene oxide nanoribbons in chitosan
BODIPY: Borondipyrromethene
SPCE: Screen printed carbon electrode
TNFs: titanium dioxide nanofibers
PGE: Pencil graphite electrode
GPE: Graphite paste electrode
PVIM: Poly(ionic liquid)
Poly(DA): Poly(dopamine)
Poly(HQ): Poly(hydroquinone)
β-NiS: Restacked nanosheets of nickel sulfide
Poly(BCG): poly(3,3’,5,5’-tetrabromo-mcresolsulfonphthalein)
EB-PPY: Electron beam irradiated Poly(pyrrole)
BSA: Bovine serum albumin
Poly(BCP): Poly(bromocresol purple)

Declaration of interests

The authors declare that they have no known competing financial interests or personal relationships that could have appeared to influence the work reported in this paper.
The authors declare the following financial interests/personal relationships which may be considered as potential competing interests:

8. Acknowledgements

This work was supported by NIH P20 GM113131 and NSF EPSCoR award #1757371. The authors would also like to acknowledge the support of the Surface Enhanced Electrochemical Diagnostics Sensors (SEEDS) Laboratory, Center for Integrated Biomedical and Bioengineering and the College of Engineering and Physical Sciences at University of New Hampshire.

9. References

[1] Y. Gao, L. Li, X. Zhang, X. Wang, W. Ji, J. Zhao, Y. Ozaki, CTAB-triggered Ag aggregates for reproducible SERS analysis of urinary polycyclic aromatic hydrocarbon metabolites., Chem. Commun. (Camb). 55 (2019) 2146–2149. https://doi.org/10.1039/c8cc09008d.

[2] W. Li, F. Wu, Y. Dai, J. Zhang, B. Ni, J. Wang, Poly (Octadecyl Methacrylate-Co-Trimethylolpropane Trimethacrylate) Monolithic Column for Hydrophobic in-Tube Solid-Phase Microextraction of Chlorophenoxy Acid Herbicides, Molecules. 24 (2019) 1678. https://doi.org/10.3390/molecules24091678.

[3] O. Parlak, S.T. Keene, A. Marais, V.F. Curto, A. Salleo, Molecularly selective nanoporous membrane-based wearable organic electrochemical device for noninvasive cortisol sensing, Sci. Adv. 4 (2018) eaar2904. https://doi.org/10.1126/sciadv.aar2904.

[4] M. Wei, Y. Qiao, H. Zhao, J. Liang, T. Li, Y. Luo, S. Lu, X. Shi, W. Lu, X. Sun, Electrochemical non-enzymatic glucose sensors: recent progress and perspectives, Chem. Commun. 56 (2020) 14553–14569. https://doi.org/10.1039/D0CC05650B.

[5] S. Lakard, I.-A. Pavel, B. Lakard, Electrochemical Biosensing of Dopamine Neurotransmitter: A Review, Biosensors. 11 (2021) 179. https://doi.org/10.3390/bios11060179.

[6] Y. Qiao, Q. Liu, S. Lu, G. Chen, S. Gao, W. Lu, X. Sun, High-performance non-enzymatic glucose detection: using a conductive Ni-MOF as an electrocatalyst, J. Mater. Chem. B. 8 (2020) 5411–5415. https://doi.org/10.1039/D0TB00131G.

[7] F. Xie, X. Cao, F. Qu, A.M. Asiri, X. Sun, Cobalt nitride nanowire array as an efficient electrochemical sensor for glucose and H2O2 detection, Sensors Actuators B Chem. 255 (2018) 1254–1261. https://doi.org/10.1016/j.snb.2017.08.098.

[8] M. Wei, W. Lu, M. Zhu, R. Zhang, W. Hu, X. Cao, J. Jia, H. Wu, Highly sensitive and selective dopamine sensor uses three-dimensional cobalt phosphide nanowire array, J. Mater. Sci. 56 (2021) 6401–6410. https://doi.org/10.1007/s10853-020-05713-0.

[9] S. Pradhan, S. Pramanik, Di.K. Das, R. Bhar, R. Bandyopadhyay, P. Millner, P. Pramanik, Nanosized iron telluride for simultaneous nanomolar voltammetric determination of dopamine, uric acid, guanine and adenine, New J. Chem. 43 (2019) 10590–10600. https://doi.org/10.1039/c9nj02329a.

[10] F.J. Nieto, C. Iribarren, M.D. Gross, G.W. Comstock, R.G. Cutler, Uric acid and serum antioxidant capacity: a reaction to atherosclerosis?, Atherosclerosis. 148 (2000) 131–139. https://doi.org/10.1016/S0021-9150(99)00214-2.

[11] P. Muthukumaran, C. Sumathi, J. Wilson, G. Ravi, Enzymeless biosensor based on β-NiS@rGO/Au nanocomposites for simultaneous detection of ascorbic acid, epinephrine and uric acid, RSC Adv. 6 (2016) 96467–96478. https://doi.org/10.1039/C6RA19921F.

[12] T. Zhang, X. Sun, B. Liu, Synthesis of positively charged CdTe quantum dots and detection for uric

acid, Spectrochim. Acta - Part A Mol. Biomol. Spectrosc. 79 (2011) 1566–1572. https://doi.org/10.1016/j.saa.2011.05.014.

[13] Z. Cai, Y. Ye, X. Wan, J. Liu, S. Yang, Y. Xia, G. Li, Q. He, Morphology–Dependent Electrochemical Sensing Properties of Iron Oxide–Graphene Oxide Nanohybrids for Dopamine and Uric Acid, Nanomaterials. 9 (2019) 835. https://doi.org/10.3390/nano9060835.

[14] A. Arroquia, I. Acosta, M.P.G. Armada, Self-assembled gold decorated polydopamine nanospheres as electrochemical sensor for simultaneous determination of ascorbic acid, dopamine, uric acid and tryptophan, Mater. Sci. Eng. C. 109 (2020) 110602. https://doi.org/10.1016/j.msec.2019.110602.

[15] A.C. Anithaa, K. Asokan, C. Sekar, Voltammetric determination of epinephrine and xanthine based on sodium dodecyl sulphate assisted tungsten trioxide nanoparticles, Electrochim. Acta. 237 (2017) 44–53. https://doi.org/10.1016/j.electacta.2017.03.098.

[16] S. Bonyadi, K. Ghanbari, M. Ghiasi, All-electrochemical synthesis of a three-dimensional mesoporous polymeric g-C 3 N 4 /PANI/CdO nanocomposite and its application as a novel sensor for the simultaneous determination of epinephrine, paracetamol, mefenamic acid, and ciprofloxacin, New J. Chem. 44 (2020) 3412–3424. https://doi.org/10.1039/C9NJ05954G.

[17] W. Dong, Y. Ren, Z. Bai, J. Jiao, Y. Chen, B. Han, Q. Chen, Synthesis of tetrahexahedral Au-Pd core–shell nanocrystals and reduction of graphene oxide for the electrochemical detection of epinephrine, J. Colloid Interface Sci. 512 (2018) 812–818. https://doi.org/10.1016/j.jcis.2017.10.071.

[18] A. Gorczyński, M. Kubicki, K. Szymkowiak, T. Łuczak, V. Patroniak, Utilization of a new gold/Schiff-base iron(iii) complex composite as a highly sensitive voltammetric sensor for determination of epinephrine in the presence of ascorbic acid, RSC Adv. 6 (2016) 101888–101899. https://doi.org/10.1039/c6ra22028b.

[19] D.Y. Lee, E. Kim, M.H. Choi, Technical and clinical aspects of cortisol as a biochemical marker of chronic stress, BMB Rep. 48 (2015) 209–216. https://doi.org/10.5483/BMBRep.2015.48.4.275.

[20] E. Wierzbicka, M. Szultka-Młyńska, B. Buszewski, G.D. Sulka, Epinephrine sensing at nanostructured Au electrode and determination its oxidative metabolism, Sensors Actuators B Chem. 237 (2016) 206–215. https://doi.org/10.1016/j.snb.2016.06.073.

[21] E. Fries, J. Hesse, J. Hellhammer, D.H. Hellhammer, A new view on hypocortisolism, Psychoneuroendocrinology. 30 (2005) 1010–1016. https://doi.org/10.1016/j.psyneuen.2005.04.006.

[22] M. Sekar, M. Pandiaraj, S. Bhansali, N. Ponpandian, C. Viswanathan, Carbon fiber based electrochemical sensor for sweat cortisol measurement, Sci. Rep. 9 (2019) 1–14. https://doi.org/10.1038/s41598-018-37243-w.

[23] K.S. Kim, S.R. Lim, S.-E. Kim, J.Y. Lee, C.-H. Chung, W.-S. Choe, P.J. Yoo, Highly sensitive and selective electrochemical cortisol sensor using bifunctional protein interlayer-modified graphene electrodes, Sensors Actuators B Chem. 242 (2017) 1121–1128. https://doi.org/10.1016/j.snb.2016.09.135.

[24] M. Zea, F.G. Bellagambi, H. Ben Halima, N. Zine, N. Jaffrezic-Renault, R. Villa, G. Gabriel, A. Errachid, Electrochemical sensors for cortisol detections: Almost there, TrAC Trends Anal. Chem. (2020) 116058.

[25] V. Narwal, R. Deswal, B. Batra, V. Kalra, R. Hooda, M. Sharma, J.S. Rana, Cholesterol biosensors: A review, Steroids. 143 (2019) 6–17. https://doi.org/10.1016/j.steroids.2018.12.003.

[26] F.J. van Spronsen, M. van Rijn, J. Bekhof, R. Koch, P.G.A. Smit, Phenylketonuria: tyrosine supplementation in phenylalanine-restricted diets, Am. J. Clin. Nutr. 73 (2001) 153–157. https://doi.org/10.1093/ajcn/73.2.153.

[27] Z. Wei, Electrochemical Determination of Tyrosine in Human Serum Based on Glycine Polymer and Multi-walled Carbon Nanotubes Modified Carbon Paste Electrode, Int. J. Electrochem. Sci. 13 (2018) 7478–7488. https://doi.org/10.20964/2018.08.26.

[28] G. Desideri, G. Castaldo, A. Lombardi, M. Mussap, A. Testa, R. Pontremoli, L. Punzi, C. Borghi, Is it time to revise the normal range of serum uric acid levels?, Eur. Rev. Med. Pharmacol. Sci. 18 (2014) 1295–1306. http://www.ncbi.nlm.nih.gov/pubmed/24867507.

[29] Y. Kumar, S. Pradhan, S. Pramanik, R. Bandyopadhyay, D.K. Das, P. Pramanik, Efficient electrochemical detection of guanine, uric acid and their mixture by composite of nano-particles of lanthanides ortho-ferrite XFeO3 (X = La, Gd, Pr, Dy, Sm, Ce and Tb), J. Electroanal. Chem. 830–831 (2018) 95–105. https://doi.org/10.1016/j.jelechem.2018.10.021.

[30] C.C. Chernecky, B.J. Berger, Laboratory Tests and Diagnostic Procedures, 6 Edition, Elsevier, St. Louis, 2013.

[31] C.-L. Lin, T.-J. Wu, D.A. Machacek, N.-S. Jiang, P.C. Kao, Urinary Free Cortisol and Cortisone Determined by High Performance Liquid Chromatography in the Diagnosis of Cushing's Syndrome, J. Clin. Endocrinol. Metab. 82 (1997) 151–155. https://doi.org/10.1210/jcem.82.1.3687.

[32] E. Aardal, A.C. Holm, Cortisol in Saliva — Reference Ranges and Relation to Cortisol in Serum, Clin. Chem. Lab. Med. 33 (1995) 927–932. https://doi.org/10.1515/cclm.1995.33.12.927.

[33] T.W. Traut, Physiological concentrations of purines and pyrimidines, Mol. Cell. Biochem. 140 (1994) 1–22. https://doi.org/10.1007/BF00928361.

[34] W.A. Adeosun, A.M. Asiri, H.M. Marwani, M.M. Rahman, Enzymeless Electrocatalytic Detection of Uric Acid Using Polydopamine/Polypyrrole Copolymeric film, ChemistrySelect. 5 (2020) 156–164. https://doi.org/10.1002/slct.201903628.

[35] D. Zhu, H. Ma, Q. Zhen, J. Xin, L. Tan, C. Zhang, X. Wang, B. Xiao, Hierarchical flower-like zinc oxide nanosheets in-situ growth on three-dimensional ferrocene-functionalized graphene framework for sensitive determination of epinephrine and its oxidation derivative, Appl. Surf. Sci. 526 (2020) 146721. https://doi.org/10.1016/j.apsusc.2020.146721.

[36] S. Rison, K.B. Akshaya, V.S. Bhat, G. Shanker, T. Maiyalagan, E.K. Joice, G. Hegde, A. Varghese, MnO 2 Nanoclusters Decorated on GrapheneModified Pencil Graphite Electrode for Non-Enzymatic Determination of Cholesterol, Electroanalysis. 32 (2020) 2128–2136. https://doi.org/10.1002/elan.202000049.

[37] A. Karthika, D.R. Rosaline, S.S.R. Inbanathan, A. Suganthi, M. Rajarajan, Fabrication of Cupric oxide decorated β-cyclodextrin nanocomposite solubilized Nafion as a high performance electrochemical sensor for l-tyrosine detection, J. Phys. Chem. Solids. 136 (2020) 109145. https://doi.org/10.1016/j.jpcs.2019.109145.

[38] J. Zhou, S. Li, M. Noroozifar, K. Kerman, Graphene Oxide Nanoribbons in Chitosan for Simultaneous Electrochemical Detection of Guanine, Adenine, Thymine and Cytosine, Biosensors. 10 (2020) 30.

https://doi.org/10.3390/bios10040030.

[39] R. Sheng, F. Ni, T.M. Cotton, Determination of purine bases by reversed-phase high-performance liquid chromatography using real-time surface-enhanced Raman spectroscopy, Anal. Chem. 63 (1991) 437–442. https://doi.org/10.1021/ac00005a010.

[40] K. Shrivas, N. Nirmalkar, S.S. Thakur, R. Kurrey, D. Sinha, R. Shankar, Experimental and theoretical approaches for the selective detection of thymine in real samples using gold nanoparticles as a biochemical sensor, RSC Adv. 8 (2018) 24328–24337. https://doi.org/10.1039/C8RA02627K.

[41] V. Sharma, F. Jelen, L. Trnkova, Functionalized Solid Electrodes for Electrochemical Biosensing of Purine Nucleobases and Their Analogues: A Review, Sensors. 15 (2015) 1564–1600. https://doi.org/10.3390/s150101564.

[42] P.L. Clark, K.G. Ugrinov, Chapter 24 Measuring Cotranslational Folding of Nascent Polypeptide Chains on Ribosomes, in: Methods Enzymol., Elsevier, 2009: pp. 567–590. https://doi.org/10.1016/S0076-6879(09)66024-9.

[43] K. Scott, Electrochemical principles and characterization of bioelectrochemical systems, in: Microb. Electrochem. Fuel Cells, Elsevier, 2016: pp. 29–66. https://doi.org/10.1016/B978-1-78242-375-1.00002-2.

[44] G. Zhu, L. Wu, X. Zhang, W. Liu, X. Zhang, J. Chen, A New Dual-Signalling Electrochemical Sensing Strategy Based on Competitive Host-Guest Interaction of a β-Cyclodextrin/Poly(N -acetylaniline)/Graphene-Modified Electrode: Sensitive Electrochemical Determination of Organic Pollutants, Chem. - A Eur. J. 19 (2013) 6368–6373. https://doi.org/10.1002/chem.201204635.

[45] S. Alexander, P. Baraneedharan, S. Balasubrahmanyan, S. Ramaprabhu, Modified graphene based molecular imprinted polymer for electrochemical non-enzymatic cholesterol biosensor, Eur. Polym. J. 86 (2017) 106–116. https://doi.org/10.1016/j.eurpolymj.2016.11.024.

[46] M.A.H. Nawaz, M. Majdinasab, U. Latif, M. Nasir, G. Gokce, M.W. Anwar, A. Hayat, Development of a disposable electrochemical sensor for detection of cholesterol using differential pulse voltammetry, J. Pharm. Biomed. Anal. 159 (2018) 398–405. https://doi.org/10.1016/j.jpba.2018.07.005.

[47] L. Yang, H. Zhao, S. Fan, G. Zhao, X. Ran, C.-P. Li, Electrochemical detection of cholesterol based on competitive host–guest recognition using a β-cyclodextrin/poly(N-acetylaniline)/graphene-modified electrode, RSC Adv. 5 (2015) 64146–64155. https://doi.org/10.1039/C5RA11420A.

[48] S. Kämäräinen, M. Mäki, T. Tolonen, G. Palleschi, V. Virtanen, L. Micheli, A.M. Sesay, Disposable electrochemical immunosensor for cortisol determination in human saliva, Talanta. 188 (2018) 50–57. https://doi.org/10.1016/j.talanta.2018.05.039.

[49] A. Salimi, R. Hallaj, G.R. Khayatian, Amperometric detection of morphine at preheated glassy carbon electrode modified with multiwall carbon nanotubes, Electroanalysis. 17 (2005) 873–879. https://doi.org/10.1002/elan.200403166.

[50] J.L. Hammond, N. Formisano, P. Estrela, S. Carrara, J. Tkac, Electrochemical biosensors and nanobiosensors, Essays Biochem. 60 (2016) 69–80. https://doi.org/10.1042/EBC20150008.

[51] J. Salamon, Y. Sathishkumar, K. Ramachandran, Y.S. Lee, D.J. Yoo, A.R. Kim, G. Gnana kumar, One-pot synthesis of magnetite nanorods/graphene composites and its catalytic activity toward electrochemical detection of dopamine, Biosens. Bioelectron. 64 (2015) 269–276. https://doi.org/10.1016/j.bios.2014.08.085.

[52] A. Fiorani, J.P. Merino, A. Zanut, A. Criado, G. Valenti, M. Prato, F. Paolucci, Advanced carbon nanomaterials for electrochemiluminescent biosensor applications, Curr. Opin. Electrochem. 16 (2019) 66–74. https://doi.org/10.1016/j.coelec.2019.04.018.

[53] J.C. Ndamanisha, L. Guo, Ordered mesoporous carbon for electrochemical sensing: A review, Anal. Chim. Acta. 747 (2012) 19–28. https://doi.org/10.1016/j.aca.2012.08.032.

[54] S. Pilehvar, K. De Wael, Recent Advances in Electrochemical Biosensors Based on Fullerene-C60 Nano-Structured Platforms, Biosensors. 5 (2015) 712–735. https://doi.org/10.3390/bios5040712.

[55] Z. Lin, G. Wu, L. Zhao, K.W.C. Lai, Carbon Nanomaterial-Based Biosensors: A Review of Design and Applications, IEEE Nanotechnol. Mag. 13 (2019) 4–14. https://doi.org/10.1109/MNANO.2019.2927774.

[56] U. Kamran, Y.-J. Heo, J.W. Lee, S.-J. Park, Functionalized Carbon Materials for Electronic Devices: A Review, Micromachines. 10 (2019) 234. https://doi.org/10.3390/mi10040234.

[57] M. Sireesha, V. Jagadeesh Babu, A.S. Kranthi Kiran, S. Ramakrishna, A review on carbon nanotubes in biosensor devices and their applications in medicine, Nanocomposites. 4 (2018) 36–57. https://doi.org/10.1080/20550324.2018.1478765.

[58] S. Gupta, C.N. Murthy, C.R. Prabha, Recent advances in carbon nanotube based electrochemical biosensors, Int. J. Biol. Macromol. 108 (2018) 687–703. https://doi.org/10.1016/j.ijbiomac.2017.12.038.

[59] F. Foroughi, M. Rahsepar, H. Kim, A highly sensitive and selective biosensor based on nitrogen-doped graphene for non-enzymatic detection of uric acid and dopamine at biological pH value, J. Electroanal. Chem. 827 (2018) 34–41. https://doi.org/10.1016/j.jelechem.2018.09.008.

[60] K. Movlaee, H. Beitollahi, M.R. Ganjali, P. Norouzi, Electrochemical platform for simultaneous determination of levodopa, acetaminophen and tyrosine using a graphene and ferrocene modified carbon paste electrode, Microchim. Acta. 184 (2017) 3281–3289. https://doi.org/10.1007/s00604-017-2291-3.

[61] H. Cui, J. Zheng, Y. Zhu, Z. Wang, S. Jia, Z. Zhu, Graphene frameworks synthetized with Na2CO3 as a renewable water-soluble substrate and their high rate capability for supercapacitors, J. Power Sources. 293 (2015) 143–150. https://doi.org/10.1016/J.JPOWSOUR.2015.05.068.

[62] H.J. Cui, H.M. Yu, J.F. Zheng, Z.J. Wang, Y.Y. Zhu, S.P. Jia, J. Jia, Z.P. Zhu, N-Doped graphene frameworks with superhigh surface area: excellent electrocatalytic performance for oxygen reduction, Nanoscale. 8 (2016) 2795–2803. https://doi.org/10.1039/C5NR06319A.

[63] S. He, P. He, X. Zhang, X. Zhang, K. Liu, L. Jia, F. Dong, Poly(glycine)/graphene oxide modified glassy carbon electrode: Preparation, characterization and simultaneous electrochemical determination of dopamine, uric acid, guanine and adenine, Anal. Chim. Acta. 1031 (2018) 75–82. https://doi.org/10.1016/j.aca.2018.06.020.

[64] X. Zhang, Y.-C. Zhang, L.-X. Ma, One-pot facile fabrication of graphene-zinc oxide composite and its enhanced sensitivity for simultaneous electrochemical detection of ascorbic acid, dopamine and uric acid, Sensors Actuators B Chem. 227 (2016) 488–496. https://doi.org/10.1016/j.snb.2015.12.073.

[65] B. Sun, Y. Gou, Y. Ma, X. Zheng, R. Bai, A.A. Ahmed Abdelmoaty, F. Hu, Investigate electrochemical immunosensor of cortisol based on gold nanoparticles/magnetic functionalized reduced graphene oxide, Biosens. Bioelectron. 88 (2017) 55–62.

https://doi.org/10.1016/j.bios.2016.07.047.

[66] M. Arvand, N. Ghodsi, M.A. Zanjanchi, A new microplatform based on titanium dioxide nanofibers/graphene oxide nanosheets nanocomposite modified screen printed carbon electrode for electrochemical determination of adenine in the presence of guanine, Biosens. Bioelectron. 77 (2016) 837–844. https://doi.org/10.1016/j.bios.2015.10.055.

[67] Z. Zhu, An Overview of Carbon Nanotubes and Graphene for Biosensing Applications, Nano-Micro Lett. 9 (2017) 25. https://doi.org/10.1007/s40820-017-0128-6.

[68] J. Chen, P. He, H. Bai, S. He, T. Zhang, X. Zhang, F. Dong, Poly(B-cyclodextrin)/carbon quantum dots modified glassy carbon electrode: Preparation, characterization and simultaneous electrochemical determination of dopamine, uric acid and tryptophan, Sensors Actuators, B Chem. 252 (2017) 9–16. https://doi.org/10.1016/j.snb.2017.05.096.

[69] S. Dong, Q. Bi, C. Qiao, Y. Sun, X. Zhang, X. Lu, L. Zhao, Electrochemical sensor for discrimination tyrosine enantiomers using graphene quantum dots and β-cyclodextrins composites, Talanta. 173 (2017) 94–100. https://doi.org/10.1016/j.talanta.2017.05.045.

[70] T.C. Canevari, M. Nakamura, F.H. Cincotto, F.M. De Melo, H.E. Toma, High performance electrochemical sensors for dopamine and epinephrine using nanocrystalline carbon quantum dots obtained under controlled chronoamperometric conditions, Electrochim. Acta. 209 (2016) 464–470. https://doi.org/10.1016/j.electacta.2016.05.108.

[71] S.E. Elugoke, A.S. Adekunle, O.E. Fayemi, B.B. Mamba, E.S.M. Sherif, E.E. Ebenso, Carbon-Based Quantum Dots for Electrochemical Detection of Monoamine Neurotransmitters—Review, Biosensors. 10 (2020) 162. https://doi.org/10.3390/bios10110162.

[72] A. Sanati, M. Jalali, K. Raeissi, F. Karimzadeh, M. Kharaziha, S.S. Mahshid, S. Mahshid, A review on recent advancements in electrochemical biosensing using carbonaceous nanomaterials, Microchim. Acta. 186 (2019) 773. https://doi.org/10.1007/s00604-019-3854-2.

[73] M.B. Wayu, M.A. Schwarzmann, S.D. Gillespie, M.C. Leopold, Enzyme-free uric acid electrochemical sensors using β-cyclodextrin-modified carboxylic acid-functionalized carbon nanotubes, J. Mater. Sci. 52 (2017) 6050–6062. https://doi.org/10.1007/s10853-017-0844-9.

[74] L. García-Carmona, M. Moreno-Guzmán, T. Sierra, M.C. González, A. Escarpa, Filtered carbon nanotubes-based electrodes for rapid sensing and monitoring of L-tyrosine in plasma and whole blood samples, Sensors Actuators B Chem. 259 (2018) 762–767. https://doi.org/10.1016/j.snb.2017.12.090.

[75] O.J. D'Souza, R.J. Mascarenhas, A.K. Satpati, L. V Aiman, Z. Mekhalif, Electrocatalytic oxidation of l-tyrosine at carboxylic acid functionalized multi-walled carbon nanotubes modified carbon paste electrode, Ionics (Kiel). 22 (2016) 405–414. https://doi.org/10.1007/s11581-015-1552-6.

[76] H. Sarıoğulları, A. Şenocak, T. Basova, E. Demirbaş, M. Durmuş, Effect of different SWCNT-BODIPY hybrid materials for selective and sensitive electrochemical detection of guanine and adenine, J. Electroanal. Chem. 840 (2019) 10–20. https://doi.org/10.1016/j.jelechem.2019.03.045.

[77] J. Zhang, D. Han, S. Wang, X. Zhang, R. Yang, Y. Ji, X. Yu, Electrochemical detection of adenine and guanine using a three-dimensional WS2 nanosheet/graphite microfiber hybrid electrode, Electrochem. Commun. 99 (2019) 75–80. https://doi.org/10.1016/j.elecom.2019.01.007.

[78] K. Wang, C. Wu, F. Wang, M. Liao, G. Jiang, Bimetallic nanoparticles decorated hollow nanoporous carbon framework as nanozyme biosensor for highly sensitive electrochemical sensing of uric

acid, Biosens. Bioelectron. 150 (2020) 111869. https://doi.org/10.1016/j.bios.2019.111869.

[79] M. Taleb, R. Ivanov, S. Bereznev, S.H. Kazemi, I. Hussainova, Alumina/graphene/Cu hybrids as highly selective sensor for simultaneous determination of epinephrine, acetaminophen and tryptophan in human urine, J. Electroanal. Chem. 823 (2018) 184–192. https://doi.org/10.1016/j.jelechem.2018.06.013.

[80] Q. Wang, J. Zhang, Q. Li, X. Guo, L. Zhang, Fabrication of WO2/W@C core-shell nanospheres for voltammetric simultaneous determination of thymine and cytosine, Microchim. Acta. 187 (2020) 62. https://doi.org/10.1007/s00604-019-3987-3.

[81] M.M. Alam, M.T. Uddin, A.M. Asiri, M.M. Rahman, M.A. Islam, Detection of L-Tyrosine by electrochemical method based on binary mixed CdO/SnO2 nanoparticles, Measurement. 163 (2020) 107990. https://doi.org/10.1016/j.measurement.2020.107990.

[82] N.F.B. Azeredo, J.M. Gonçalves, P.O. Rossini, K. Araki, J. Wang, L. Angnes, Uric acid electrochemical sensing in biofluids based on Ni/Zn hydroxide nanocatalyst, Microchim. Acta. 187 (2020) 379. https://doi.org/10.1007/s00604-020-04351-2.

[83] C. Tooley, C. Gasperoni, S. Marnoto, J. Halpern, Evaluation of Metal Oxide Surface Catalysts for the Electrochemical Activation of Amino Acids, Sensors. 18 (2018) 3144. https://doi.org/10.3390/s18093144.

[84] S. Hooshmand, Z. Es'haghi, Microfabricated disposable nanosensor based on CdSe quantum dot/ionic liquid-mediated hollow fiber-pencil graphite electrode for simultaneous electrochemical quantification of uric acid and creatinine in human samples, Anal. Chim. Acta. 972 (2017) 28–37. https://doi.org/10.1016/j.aca.2017.04.035.

[85] Ö.A. Yokuş, F. Kardaş, O. Akyıldırım, T. Eren, N. Atar, M.L. Yola, Sensitive voltammetric sensor based on polyoxometalate/reduced graphene oxide nanomaterial: Application to the simultaneous determination of l-tyrosine and l-tryptophan, Sensors Actuators B Chem. 233 (2016) 47–54. https://doi.org/10.1016/j.snb.2016.04.050.

[86] N. Thakur, M. Kumar, S. Das Adhikary, D. Mandal, T.C. Nagaiah, PVIM–Co 5 POM/MNC composite as a flexible electrode for the ultrasensitive and highly selective non-enzymatic electrochemical detection of cholesterol, Chem. Commun. 55 (2019) 5021–5024. https://doi.org/10.1039/C9CC01534E.

[87] A.E. Martell, Metal-Catalyzed Reactions of Organic Compounds, in: Chem. Chang. Food Dur. Process., Springer Netherlands, Dordrecht, 1985: pp. 33–61. https://doi.org/10.1007/978-94-017-1016-9_3.

[88] M. Arvand, Z. Khoshkholgh, S. Hemmati, Trace level detection of guanine and adenine and evaluation of damage to DNA using electro-synthesised ZnS@CdS core-shell quantum dots decorated graphene oxide nanocomposite, J. Electroanal. Chem. 817 (2018) 149–159. https://doi.org/10.1016/j.jelechem.2018.04.010.

[89] Q. Xie, X. Chen, H. Zhang, M. Liu, Q. Wang, X. Zhang, Y. Shen, F. Yang, Fabrication of a Modified Electrode Based on Fe 3 O 4 -Graphene Oxide Hybrid Composite: Applying to Simultaneous Determination of Adenine and Guanine in DNA, Electroanalysis. 27 (2015) 2201–2208. https://doi.org/10.1002/elan.201500186.

[90] Z. Cai, Y. Ye, X. Wan, J. Liu, S. Yang, Y. Xia, G. Li, Q. He, Morphology–Dependent Electrochemical Sensing Properties of Iron Oxide–Graphene Oxide Nanohybrids for Dopamine and Uric Acid,

Nanomaterials. 9 (2019) 835. https://doi.org/10.3390/nano9060835.

[91] P.S. Adarakatti, M. Mahanthappa, H. Eranjaneya, A. Siddaramanna, Fe2V4O13 Nanoparticles Based Electrochemical Sensor for the Simultaneous Determination of Guanine and Adenine at Nanomolar Concentration, Electroanalysis. 30 (2018) 1971–1982. https://doi.org/10.1002/elan.201800124.

[92] L.E. Kreno, K. Leong, O.K. Farha, M. Allendorf, R.P. Van Duyne, J.T. Hupp, Metal–Organic Framework Materials as Chemical Sensors, Chem. Rev. 112 (2012) 1105–1125. https://doi.org/10.1021/cr200324t.

[93] M. Ammam, Polyoxometalates: formation, structures, principal properties, main deposition methods and application in sensing, J. Mater. Chem. A. 1 (2013) 6291. https://doi.org/10.1039/c3ta01663c.

[94] M. Rahman, P. Kumar, D.-S. Park, Y.-B. Shim, Electrochemical Sensors Based on Organic Conjugated Polymers, Sensors. 8 (2008) 118–141. https://doi.org/10.3390/s8010118.

[95] U. Lange, N. V. Roznyatovskaya, V.M. Mirsky, Conducting polymers in chemical sensors and arrays, Anal. Chim. Acta. 614 (2008) 1–26. https://doi.org/10.1016/j.aca.2008.02.068.

[96] S. Shrestha, R.J. Mascarenhas, O.J. D'Souza, A.K. Satpati, Z. Mekhalif, A. Dhason, P. Martis, Amperometric sensor based on multi-walled carbon nanotube and poly (Bromocresol purple) modified carbon paste electrode for the sensitive determination of L-tyrosine in food and biological samples, J. Electroanal. Chem. 778 (2016) 32–40. https://doi.org/10.1016/j.jelechem.2016.08.010.

[97] N.F. Atta, A. Galal, A.R. El-Gohary, Crown ether modified poly(hydroquinone)/carbon nanotubes based electrochemical sensor for simultaneous determination of levodopa, uric acid, tyrosine and ascorbic acid in biological fluids, J. Electroanal. Chem. 863 (2020) 114032. https://doi.org/10.1016/j.jelechem.2020.114032.

[98] B. Mekassa, M. Tessema, B.S. Chandravanshi, P.G.L. Baker, F.N. Muya, Sensitive electrochemical determination of epinephrine at poly(L-aspartic acid)/electro-chemically reduced graphene oxide modified electrode by square wave voltammetry in pharmaceutics, J. Electroanal. Chem. 807 (2017) 145–153. https://doi.org/10.1016/j.jelechem.2017.11.045.

[99] T. Yang, R. Yang, H. Chen, F. Nan, T. Ge, K. Jiao, Electrocatalytic Activity of Molybdenum Disulfide Nanosheets Enhanced by Self-Doped Polyaniline for Highly Sensitive and Synergistic Determination of Adenine and Guanine, ACS Appl. Mater. Interfaces. 7 (2015) 2867–2872. https://doi.org/10.1021/am5081716.

[100] A. Özcan, S. İlkbaş, Preparation of poly(3,4-ethylenedioxythiophene) nanofibers modified pencil graphite electrode and investigation of over-oxidation conditions for the selective and sensitive determination of uric acid in body fluids, Anal. Chim. Acta. 891 (2015) 312–320. https://doi.org/10.1016/j.aca.2015.08.015.

[101] R. Ramya, P. Muthukumaran, J. Wilson, Electron beam-irradiated polypyrrole decorated with Bovine serum albumin pores: Simultaneous determination of epinephrine and L-tyrosine, Biosens. Bioelectron. 108 (2018) 53–61. https://doi.org/10.1016/j.bios.2018.02.044.

[102] P. Muthukumaran, R. Ramya, P. Thivya, J. Wilson, G. Ravi, Nanocomposite based on restacked crystallites of β-NiS and Ppy for the determination of theophylline and uric acid on screen-printed electrodes, New J. Chem. 43 (2019) 19397–19407. https://doi.org/10.1039/C9NJ04246F.

[103] P. Thivya, R. Ramya, J. Wilson, Poly(3,4-ethylenedioxythiophene)/taurine biocomposite on screen printed electrode: Non-enzymatic cholesterol biosensor, Microchem. J. 157 (2020) 105037. https://doi.org/10.1016/j.microc.2020.105037.

[104] N. Dhananjayan, W. Jeyaraj, G. Karuppasamy, Interactive Studies on Synthetic Nanopolymer decorated with Edible Biopolymer and its Selective Electrochemical determination of L-Tyrosine, Sci. Rep. 9 (2019) 13287. https://doi.org/10.1038/s41598-019-49735-4.

[105] M. Wang, M. Cui, W. Liu, X. Liu, Highly dispersed conductive polypyrrole hydrogels as sensitive sensor for simultaneous determination of ascorbic acid, dopamine and uric acid, J. Electroanal. Chem. 832 (2019) 174–181. https://doi.org/10.1016/j.jelechem.2018.10.057.

[106] S. Sen, P. Sarkar, A simple electrochemical approach to fabricate functionalized MWCNT-nanogold decorated PEDOT nanohybrid for simultaneous quantification of uric acid, xanthine and hypoxanthine, Anal. Chim. Acta. 1114 (2020) 15–28. https://doi.org/10.1016/j.aca.2020.03.060.

[107] K. Ghanbari, M. Moloudi, Flower-like ZnO decorated polyaniline/reduced graphene oxide nanocomposites for simultaneous determination of dopamine and uric acid, Anal. Biochem. 512 (2016) 91–102. https://doi.org/10.1016/j.ab.2016.08.014.

[108] X. Wang, Y. Zheng, L. Xu, An electrochemical adenine sensor employing enhanced three-dimensional conductivity and molecularly imprinted sites of Au NPs bridged poly(3-thiophene acetic acid), Sensors Actuators B Chem. 255 (2018) 2952–2958. https://doi.org/10.1016/j.snb.2017.09.116.

[109] Q. Qin, X. Bai, Z. Hua, Electropolymerization of a conductive β-cyclodextrin polymer on reduced graphene oxide modified screen-printed electrode for simultaneous determination of ascorbic acid, dopamine and uric acid, J. Electroanal. Chem. 782 (2016) 50–58. https://doi.org/10.1016/j.jelechem.2016.10.004.

[110] K. Ghanbari, A. Hajian, Electrochemical characterization of Au/ZnO/PPy/RGO nanocomposite and its application for simultaneous determination of ascorbic acid, epinephrine, and uric acid, J. Electroanal. Chem. 801 (2017) 466–479. https://doi.org/10.1016/j.jelechem.2017.07.024.

[111] M. Taei, H. Hadadzadeh, F. Hasanpour, N. Tavakkoli, M.H. Dolatabadi, Simultaneous electrochemical determination of ascorbic acid, epinephrine, and uric acid using a polymer film-modified electrode based on Au nanoparticles/poly(3,3',5,5'-tetrabromo-m-cresolsulfonphthalein), Ionics (Kiel). 21 (2015) 3267–3278. https://doi.org/10.1007/s11581-015-1515-y.

[112] J.M. Baricaua, J.N. Balitaan, K.S. Santiago, P2EC.25 - Conducting polyaniline/reduced graphene oxide-modified carbon paste electrode for the electrochemical multidetection of ascorbic acid and uric acid, in: Proc. IMCS 2018, AMA Service GmbH, Von-Münchhausen-Str. 49, 31515 Wunstorf, Germany, 2018: pp. 745–746. https://doi.org/10.5162/IMCS2018/P2EC.25.

[113] D. Li, M. Liu, Y. Zhan, Q. Su, Y. Zhang, D. Zhang, Electrodeposited poly(3,4-ethylenedioxythiophene) doped with graphene oxide for the simultaneous voltammetric determination of ascorbic acid, dopamine and uric acid, Microchim. Acta. 187 (2020) 94. https://doi.org/10.1007/s00604-019-4083-4.

[114] W. Sroysee, S. Chairam, M. Amatatongchai, P. Jarujamrus, S. Tamuang, S. Pimmongkol, L. Chaicharoenwimolkul, E. Somsook, Poly(m -ferrocenylaniline) modified carbon nanotubes-paste electrode encapsulated in nafion film for selective and sensitive determination of dopamine and uric acid in the presence of ascorbic acid, J. Saudi Chem. Soc. 22 (2018) 173–182. https://doi.org/10.1016/j.jscs.2016.02.003.

[115] E. ZOR, Reduced Graphene Oxide/α-Cyclodextrin-Based Electrochemical Sensor: Characterization and Simultaneous Detection of Adenine, Guanine and Thymine, Süleyman Demirel Üniversitesi Fen Bilim.

Enstitüsü Derg. 21 (2016) 146. https://doi.org/10.19113/sdufbed.72272.

[116] M.B. Wayu, L.T. DiPasquale, M.A. Schwarzmann, S.D. Gillespie, M.C. Leopold, Electropolymerization of β-cyclodextrin onto multi-walled carbon nanotube composite films for enhanced selective detection of uric acid, J. Electroanal. Chem. 783 (2016) 192–200. https://doi.org/10.1016/j.jelechem.2016.11.021.

[117] N. Shadjou, M. Hasanzadeh, F. Talebi, Graphene Quantum Dots Incorporated into β-cyclodextrin: a Novel Polymeric Nanocomposite for Non-Enzymatic Sensing of L-Tyrosine at Physiological pH, J. Anal. Chem. 73 (2018) 602–612. https://doi.org/10.1134/S1061934818060096.

[118] S.J. Willyam, E. Saepudin, T.A. Ivandini, β-Cyclodextrin/Fe 3 O 4 nanocomposites for an electrochemical non-enzymatic cholesterol sensor, Anal. Methods. 12 (2020) 3454–3461. https://doi.org/10.1039/D0AY00933D.

[119] N. Agnihotri, A.D. Chowdhury, A. De, Non-enzymatic electrochemical detection of cholesterol using β-cyclodextrin functionalized graphene, Biosens. Bioelectron. 63 (2015) 212–217. https://doi.org/10.1016/j.bios.2014.07.037.

[120] Z. Panahi, M.A. Merrill, J.M. Halpern, Reusable Cyclodextrin-Based Electrochemical Platform for Detection of trans -Resveratrol, ACS Appl. Polym. Mater. 2 (2020) 5086–5093. https://doi.org/10.1021/acsapm.0c00866.

[121] M.A. Morales, J.M. Halpern, Guide to Selecting a Biorecognition Element for Biosensors, Bioconjug. Chem. 29 (2018) 3231–3239. https://doi.org/10.1021/acs.bioconjchem.8b00592.

[122] D.A. Armbruster, T. Pry, Limit of blank, limit of detection and limit of quantitation., Clin. Biochem. Rev. 29 Suppl 1 (2008) S49-52. http://www.ncbi.nlm.nih.gov/pubmed/18852857.

[123] S. Rison, K.B. Akshaya, V.S. Bhat, G. Shanker, T. Maiyalagan, E.K. Joice, G. Hegde, A. Varghese, MnO_2 Nanoclusters Decorated on GrapheneModified Pencil Graphite Electrode for Non-Enzymatic Determination of Cholesterol, Electroanalysis. (2020) elan.202000049. https://doi.org/10.1002/elan.202000049.

[124] G.L. Long, J.D. Winefordner, Limit of Detection A Closer Look at the IUPAC Definition, Anal. Chem. 55 (1983) 712A-724A. https://doi.org/10.1021/ac00258a724.

[125] FDA, Q2B Validation of Analytical Procedures: Methodology, 1996. http://www.fda.gov/cder/guidance/index.htmorhttp://www.fda.gov/cber/guidelines.htm (accessed July 21, 2021).

[126] T. Darvishzad, T. Lubera, S.S. Kurek, Puzzling Aqueous Solubility of Guanine Obscured by the Formation of Nanoparticles, J. Phys. Chem. B. 122 (2018) 7497–7502. https://doi.org/10.1021/acs.jpcb.8b04327.

[127] W.R. Wilcox, A. Khalaf, A. Weinberger, I. Kippen, J.R. Klinenberg, Solubility of uric acid and monosodium urate, Med. Biol. Eng. 10 (1972) 522–531. https://doi.org/10.1007/BF02474201.

[128] F. Crea, C. De Stefano, A. Irto, G. Lando, S. Materazzi, D. Milea, A. Pettignano, S. Sammartano, Understanding the Solution Behavior of Epinephrine in the Presence of Toxic Cations: A Thermodynamic Investigation in Different Experimental Conditions, Molecules. 25 (2020) 511. https://doi.org/10.3390/molecules25030511.

[129] R. Carta, G. Tola, Solubilities of L-Cystine, L-Tyrosine, L-Leucine, and Glycine in Aqueous Solutions at Various pHs and NaCl Concentrations, J. Chem. Eng. Data. 41 (1996) 414–417. https://doi.org/10.1021/je9501853.